890

PROPOSAL FOR STAGED PLASMA WAKE-FIELD ACCELERATOR EXPERIMENT AT THE FERMILAB TEST FACILITY

J. Rosenzweig* , N. Barov, E. Colby§ and L. Serafini•
UCLA Dept. of Physics and Astronomy

A. Melissinos, N. Bigelow, A. Fry and M. Fitch
University of Rochester Dept. of Physics

P. Colestock** and R. Noble
Fermi National Accelerator Laboratory

September 25, 1996

---

* Spokesman
§ Also at Fermi National Accelerator Laboratory.
• Permanent address: Instituto Nazionale di Fisica Nucleare — Milano.
** Deputy Spokesman, Fermi National Accelerator Laboratory.

TABLE OF CONTENTS

I. INTRODUCTION

This document describes a series of experiments that we propose to conduct at the Fermilab Test Facility (FTF) on the physics and engineering of plasma wake-field acceleration. This effort is an outgrowth of many ongoing efforts: the UCLA experiments on plasma wake-field acceleration presently ongoing at ANL, the Fermilab-UCLA-Rochester collaboration on the FTF, and the TESLA Test Facility (TTF) collaboration as a whole. We believe that this proposal brings together a number of goals now being pursued:

- Further development of rf photoinjector technology at Fermilab
- Research on basic physics of advanced acceleration techniques, using facilities unique to Fermilab
- Demonstration of emittance preservation in ultra-high gradient acceleration
- Demonstration of staging of advanced accelerator technique; show applicability to a linear collider.
- Strengthen existing FNAL collaborations with universities.

These goals, pursued in a timely manner, and at a relatively small additional expense compared to the investment already undertaken at the FTF. The aims of the experiments are, we believe, exciting, attractive, and of interest to both the accelerator physics and particle physics communities. This project, which represents an attempt to make a frontier advanced accelerator concept directly applicable to high energy physics, gives additional impetus and a focus for the future for the FTF, as well as basic particle accelerator research at Fermilab. We make our case in what follows.

1.1 RATIONALE FOR ADVANCED ACCELERATOR RESEARCH

The basic research, technologies and manufacturing of the next century will continue to drive society toward manipulating processes on ever larger scales with larger energies and on ever smaller scales with higher energy densities. To probe the fundamental constituents of matter, create short-wavelength radiation, induce localized nuclear, chemical and biochemical reactions, resolve objects, etch surfaces, control atoms and electrons and even fabricate nanostructures will require high energy densities but often only a limited total energy. High energy, high brightness particle beams have been one of the more successful tools of twentieth century technology. Both keV and MeV beams when produced over centimeter to meter distances provided new compact research and manufacturing tools. The creation of multi-GeV beams over distances less than a meter is now beginning. This will involve the control of energy densities at least a million times higher than in present accelerators. The forefront of this effort is the field of high gradient particle acceleration for the benefit of high energy physics. The hope is that an ultra-high energy collider could be made someday with a very short, linear accelerating structure. But like any advanced concept, high gradient acceleration may also find application in other disciplines far removed from the original field.

High gradient acceleration is by nature faced with three problems to be solved: 1) to find a suitable structure or medium to support a high electric field for accelerating test particles using immediately available power sources, 2) to find methods to manipulate and synchronize intense beams for acceleration once the high electric field is produced and 3) to develop efficient, compact power sources to couple energy from the external world to the accelerating structure, allowing staging of acceleration sections. The order of listing here is done with purpose - this is the order of technology development from previous experience in practical particle accelerators.

After more than a decade of effort, several high gradient acceleration concepts have been demonstrated with the acceleration of relatively small numbers of particles with less than the accepted notions of high beam quality - the accelerated beams typically have a large energy spread and degraded emittance. The next decade will see concentrated effort by several groups to produce high quality beams with acceleration to at least 1 GeV over several centimeters. With continuing improvements in lasers and low energy particle beams, the effort to develop efficient power sources for staged, multi-section particle accelerators has in fact already begun. In this proposal, we outline an experiment that can be performed at the (presently under construction) Fermilab Test Facility (FTF), where staging of GeV/m accelerating sections can be demonstrated for the first time, using wake-fields in plasmas driven by ultra-high brightness electron beams.

1.2 STATUS OF ADVANCED ELECTRON ACCELERATORS

A critical step in the achievement of high acceleration gradients from any one of a number of proposed electron acceleration methods now being investigated is the demonstration of good beam quality, both high intensity and low emittance, simultaneous with high acceleration gradients. Although much technological progress has been made in the last ten years or so, this goal has yet to be realized. The acceleration methods now being studied fall into two general classes: (a) laser-driven schemes which rely on the generation of accelerating fields in conjunction with plasmas or passive structures and (b) beam-driven methods which use a pump beam to generate intense accelerating wake-fields. With regard to laser accelerators in particular, the key technical issue is to generate a significant longitudinal electric field component from a nominally transverse electromagnetic wave and maintain its phase relationship with a short electron bunch for a sufficiently long time. Regarding the wake-field approach, it is necessary to devise a medium which can withstand the necessarily intense fields generated for acceleration and

simultaneously maintain beam stability - a strong wake-field coupling implies that beam-breakup and other coherent instabilities may pose a problem.

For both of these classes, a key experimental demonstration which remains to be carried out is the precise synchronization of an ultra-short bunch of electrons with the accelerating field, leading to a well-controlled beam phase space. Limits on achievable peak stored energy cause advanced accelerators to of necessity operate at short (sub-cm) wave-lengths. Thus the scale of the accelerated bunches for synchronization - commonly achieved (several mm length) low energy electron beam bunches would yield energy spreads too large for high-energy physics type uses. Many groups, including Brookhaven, UCLA, Stanford, and Los Alamos are pushing to create electron bunches one to two orders of magnitude shorter than is presently routine. Preliminary results indicate that one may expect this effort to be a success, opening the door for more serious advanced acceleration experiments.

One of the promising subclasses of the above methods is the use of plasmas to generate the accelerating fields. In the case of laser-driven approaches, plasma waves, driven to nonlinear limits by the fields of intense electron or laser beams, can provide both the accelerating gradients and transverse focusing for the accelerated particles. Significant experimental progress on the laser side has been made with resonant pumping schemes, such as the Plasma Beat Wave Accelerator (PBWA), and with nonresonant schemes such as the Laser Wake-field Accelerator (LWFA). In the beam-driven variant of this method, the Plasma Wake-field Accelerator, an excitation bunch is first used to generate the plasma waves which do the ultimate acceleration of a trailing bunch. However, for all the above plasma-based schemes, the presence of plasma in close proximity to the accelerated beam can lead to both field non-linearities and coherent instabilities which may degrade the beam quality and place a limit on beam intensity.

A proposed scheme which can overcome these problems is based on the formation of a plasma-free channel by an overdense (higher denstiy than the ambient plasma

electrons) bunch in a plasma, creating a symmetric focusing channel for the beam that is largely free of both nonlinear fields and coherent instability problems. Recent experimental work by the UCLA team at Argonne has shown the effective generation of such channels, along with a significant acceleration gradient, albeit in a poorly bunched beam.

Perhaps the most important experiment to be undertaken in this area is that of synchronization of the witness bunch with the wake-fields generated by the excitation bunch. Recently, it has been proposed that magnetic compression of an rf photoinjector beam can be applied to effectively remove the injection jitter from the witness beam that has plagued previous attempts at acceleration. The idea is that a dispersion-free chicane can be used to reduce simultaneously reduce the bunch length (to tens of microns) and the time jitter for electrons emitted from a photoinjector which simultaneously creates the drive beam. Such a scheme would enable a first real attempt at synchronization and low emittance, low energy spread acceleration - with the possibility, unique to the FTF, of staging the accelerating sections. This proof-of-principle experiment would represent a significant step forward in maturing advanced accelerator concepts.

The components of this experimental program envisioned are:

- Demonstrate synchronization of a witness beam with the beam-generated wake-fields in the blow-out regime of the PWFA, using an rf photoinjector with a bunch compression system.
- Demonstration of GeV/m acceleration.
- Understand the beam matching physics between successive modules of a multiple stage scheme. This includes the development of effective rf kickers and understanding of the associated beam dynamics.
- Demonstrate multiple stage acceleration using the PWFA; determine physics of intensity and gradient scaling, diagnose beam quality after each accelerating section.

II. NONLINEAR PLASMA WAKE-FIELD ACCELERATION

2.1 BASIC PHYSICS

Operation of the PWFA in the extremely nonlinear ("blowout", where the beam is denser than the plasma) regime was originally proposed by Rosenzweig, Breizman, Katsouleas and Su in 1991[1]. While this system is *nonlinear* from the point of view of the plasma response (all of the plasma electrons are driven out of the beam channel by the intense fields of the driving beam), it will be seen that the attributes of the accelerating and focusing fields are what accelerator physicists term *linear*. Development of this regime represents the first serious attempt at formulating a version of a plasma accelerator which has the attributes of a standard rf linear accelerator. These attributes include:

- focusing which, for electrons, is linear in offset from the symmetry axis, and independent of longitudinal position within the wave. This focusing is purely electrostatic and dependent only on the plasma ion charge density n_0,

$$F_r = -eE_r = -2\pi e^2 n_0 r \equiv -\tfrac{1}{2} m_e c^2 k_p^2 r. \tag{2.1}$$

  It should be noted that this wave is suited only for accelerating electrons, as positrons are defocused by the presence of the ion fields.

- Acceleration which is dependent only on longitudinal position within the accelerating wave, and not on transverse offset. The maximum strength of the acceleration in this regime is typically larger than the so-called wave-breaking limit

$$eE_{WB} = m_e c^2 k_p \cong \sqrt{n_0(\mathrm{cm}^{-3})}\ (\mathrm{eV/cm}). \tag{2.2}$$

  As we typically have plasma densities in the range $n_0 \approx 10^{14}$ cm^{-3}, this implies accelerating gradients in excess of 1 GeV/m.

- Operation at high gradient at mm wavelengths, due to lower plasma densities and relativistic lengthening of the plasma oscillation period. This relatively long wavelength is an advantage for beam dynamics, and the smaller plasma density mitigates transverse emittance growth due to multiple scattering of the beam off of plasma ions.

We now review the characteristics of this regime in more detail, in order to illuminate the goals of our experimental program.

Under the condition that the drive beam is much denser than the plasma, the plasma electrons are ejected from the beam channel. There are no plasma charges (except stationary ions) or currents inside of beam distribution. Once this occurs, the transverse forces are uniform in z and linear in r. The Panofsky-Wenzel theorem then states that

$$\partial_r E_z = \partial_z (E_r - H_\theta). \tag{2.3}$$

This implies that the acceleration must be independent of r, as in an m=0 TM mode traveling wave accelerator. This is in fact a profitable way of looking at the physics of the driven plasma wave's fields. There is a cavity (traveling near the speed of light!), with currents on the boundary, supporting an m=0 TM mode. Inside of this cavity, the only source is a uniform background of positive charges due to ions, which gives the linear focusing.

This regime has been studied using PIC codes (both ISIS and a new code developed by N. Barov of UCLA) and a fluid model (Breizman, *et al.*[2]). An example of the PIC code output is shown in Figure 1, where the complete rarefaction of the plasma electrons from the beam channel is displayed. While there is clearly some nonlaminarity to the plasma electron flow shown in this configuration space picture of the driven plasma wave, we have found that the fluid code has surprisingly good validity even for the very nonlinear wave motion we are considering. This is because the laminarity is maintained to a good approximation for the initial half-cycle of the wave, which is the region of our

interest, even for fields near or above the so-called wave-breaking limit. This perhaps should not be surprising because in one-dimensional relativistic plasma wave theory, wave-breaking is also suppressed and trajectories do not cross.

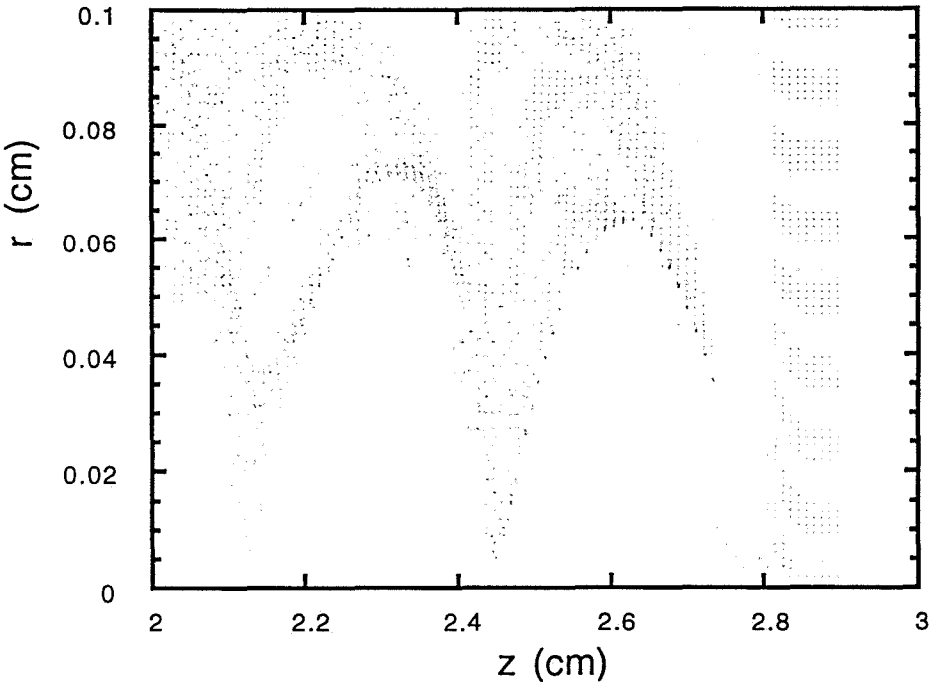

Figure 1. PIC code (N. Barov, 1995) generated distribution of plasma electrons driven into blowout oscillation by dense electron beam (not shown, moving to right). Note complete rarefaction of the beam channel.

Keeping the small reservations about the applicability of the fluid approximation in the presence of slight nonlaminarity in mind, some results from the fluid code concerning this "blow-out" regime of the PWFA are now presented. Figure 2 displays a typical case of PWFA in the blow-out regime, where a beam of twice the density (now moving to the left in the simulation) of the ambient plasma completely rarefies the beam channel, producing a pure ion channel and a nonlinear accelerating field. Figure 3 shows the dependences of the transverse and longitudinal wake-fields as a function of radius in the accelerating (for electrons) portion of the wave. It can be seen that the fields are indeed of

the form discussed above, with linear focusing no transverse dependence on the accelerating field, promising great improvements in beam quality over plasma beatwave, laser wake-field or PWFA in the linear regime. In fact, the accelerating and focusing fields in this regime are conceptually identical to a conventional linac with an applied linear focusing lattice.

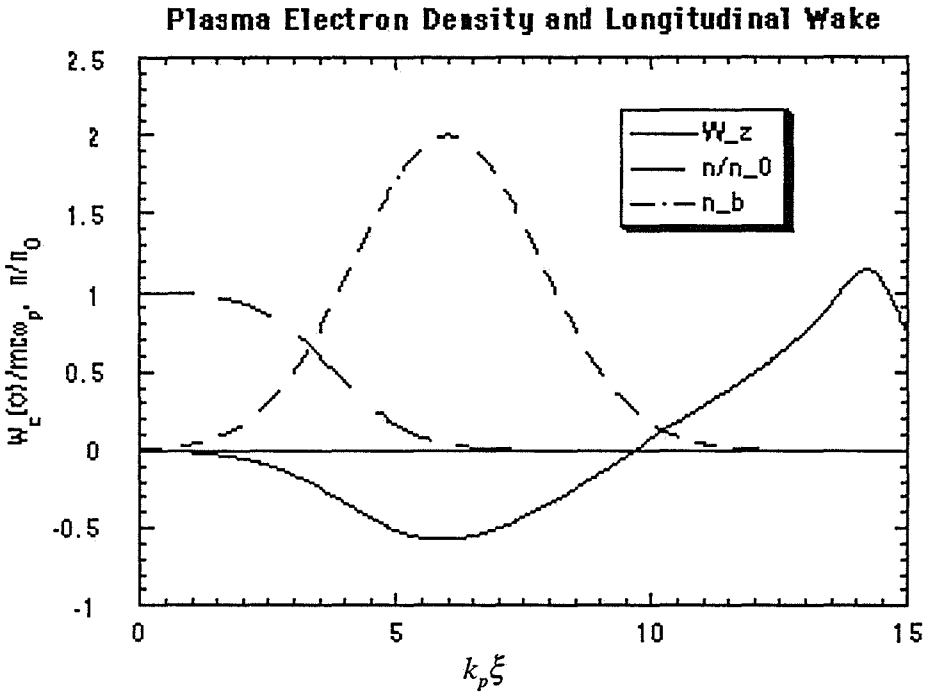

Figure 2. PWFA in the blow-out regime, beam completely rarefies plasma electrons from the beam channel. Longitudinal coordinate is stationary within the wave $\xi \equiv z - v_b t$.

The linearity of the focusing is, as stated before, due to the total rarefaction of the plasma electrons from the beam channel. This also implies other useful aspects of this system, in that beam loading within the rarefaction channel cannot change the transverse focusing, as is shown in Figure 4.

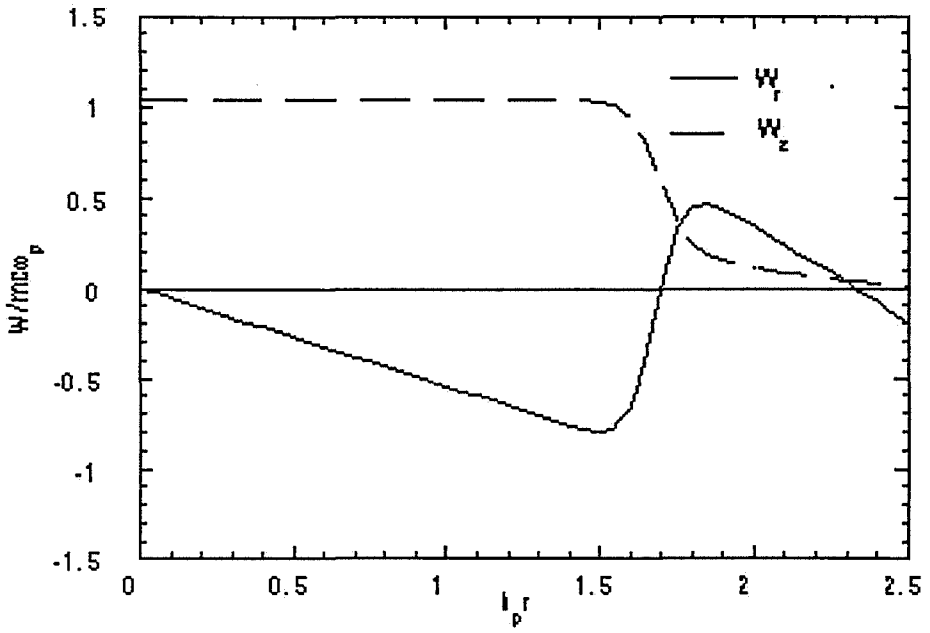

Figure 3 . Transverse and accelerating fields as a function of radius at accelerating phase of case in Figure 2, showing uniform acceleration, linear focusing within rarefaction channel.

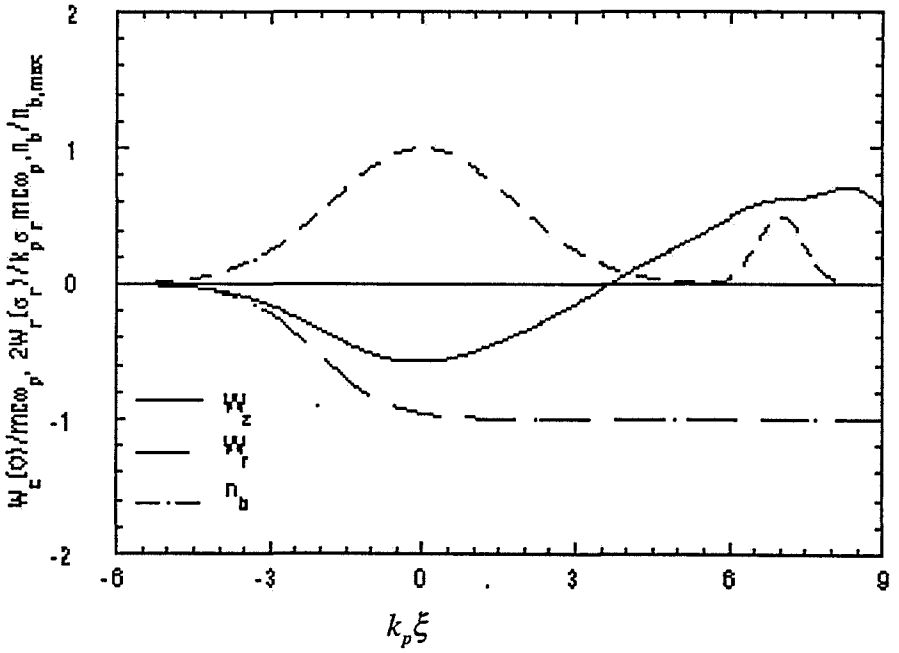

Figure 4. Wake-fields calculated at offset $k_p r = 1$; beam loading pulse centered at $k_p \xi = 1$.

Although the blow-out regime of the PWFA has significant differences with respect to the linear regime, it also retains some advantageous aspects of the linear behavior. Most notably, ramping of the drive beam on a scale length longer than k_p^{-1} allows for a transformer ratio in excess of unity, as is displayed in Figure 5. The fact that the approximately linearly ramped pulse gives this behavior in the blowout as well as linear regimes merely reflects the degree to which the plasma response can be viewed as a generalized inductance. In this view, the decelerating field inside is nearly constant $E \propto L(dI/dt)$, which is the condition found for optimum transformer ratio generation[3].

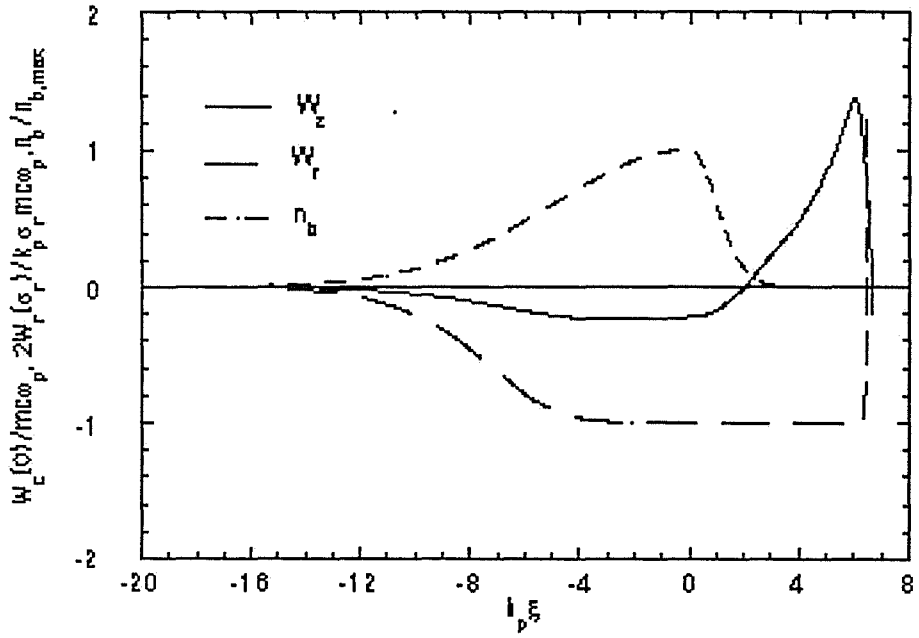

Figure 5. Drive beam ramping beam gives large transformer ratio (E_{z+} / E_{z-}).

All of the field characteristics discussed so far concern the quality of the wake-fields in the rarefaction region, where the high quality accelerating beam must be located. The transverse wake-fields for the drive beam, however, are not so uniform, because the plasma must take a finite time to respond to the beam. Because of this, the leading edge of the beam expands as if it were (ignoring small Coulomb scattering effects) in free space.

On the other hand, the main body of the drive beam can be stably matched to the uniform focusing of the electron-rarefied ion channel. If the beam density is high enough, and the emittance is low, then the erosion of the beam head is not an important effect in our experimental parameter regime.

We have explored this question in great detail, with the results applied to our experimental situation and published in a journal paper[4]. The paper presents an analytical model of how rarefaction must proceed, assuming the entire beam is in fact matched to the ion channel focusing. Given the constraint that the length of a symmetric beam must satisfy $k_p\sigma_z < 2$ (or else the wake-field behind the beam is diminished) the condition that the plasma electrons be rarefied before the arrival of the longitudinal beam center yields the constraint on the beam parameters,

$$N_b \geq \frac{9\varepsilon_n}{\sqrt{4\pi\gamma r_e}}. \tag{2.4}$$

This condition can be satisfied by rf photoinjectors, including the AWA. It is, however, a bit of an optimistic model, as beam-head erosion modifies this result. We have studied the effects of beam head erosion, as well as finite plasma density rise length with

- Maxwell-Vlasov beam/plasma electron fluid computational model.
- Superparticle beam/plasma electron fluid computational model.
- Fully self-consistent PIC code.

These studies have had a direct impact on experimental design and data interpretation. The most fundamental finding was that, while the scaling of Eq. 2.4 with emittance and energy is correct, the constant of proportionality is much larger, due to beam-head erosion effects. These results imply that one needs approximately a factor of 5 larger charge to achieve rarefaction within the drive beam.

The superparticle model has also been used to study time (propagation distance) dependent phenomena. We also have studied the following problems with this method:

- Matching. Beam can be matched more easily to the plasma focusing with a ramp in plasma density of length ~ few β^*. It should be noted in this regard that the matched β-function in the plasma

$$\beta_{eq} = \sqrt{\gamma / 2\pi r_e n_0} \tag{2.5}$$

  is quite short (a few mm in cases of present interest), a parameter indicative of the strength of the focusing required to make the beam underdense.
- Adiabatic focusing. A regime of plasma focusing in high energy physics colliders which can beat the Oide spot size limit.

The work performed by our group concerned the monopole stability (confinement) of the drive beam. It was thought several years ago that a dipole mode (the electron hose instability[5]) would cause problems for this type of PWFA, but it has been shown in 3-D simulations of short ($k_p \sigma_z < 2$), symmetric beams, that the instability has a negligibly small effect[6]. For long, ramped pulses, like that shown in Figure 4, electron hose remains a serious consideration.

The initial proposal for using the AWA to generate the drive beam in our experiments assumed an optimistic set of parameters: 100 nC of charge, rms bunch length of 0.75 mm, and normalized emittance of 400 mm-mrad. The predicted performance of this beam in a $n_0 = 2 \times 10^{14}$ cm^{-3} plasma are shown in Figure 6. The actual performance of the experiment, and reasons from the deviation from these predictions, are discussed in a following section.

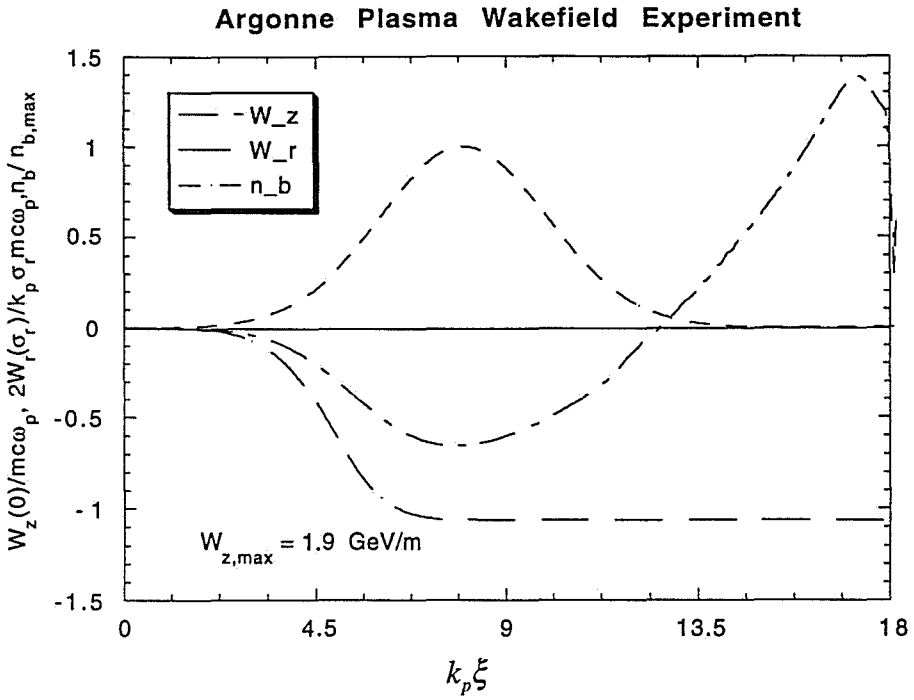

Figure 6. Original experimental parameters for the AWA nonlinear PWFA experiment, assuming $n_0 = 2\times10^{14}$ cm^{-3}.

As a final comment on the physical mechanisms in the nonlinear PWFA, we compare it (favorably) to similar schemes using laser drivers, *i.e.* LWFA. In laser based schemes, the laser needed is certainly at the edge of the state of the art, perhaps more so than the electron beam-based PWFA, especially when one considers issues of repetition rate, which lasers have serious limitations on due to material heating. It is also certain that the cost of a modular, staged accelerator is much more for the laser approach; a very inexpensive approach to the PWFA (to beam wake-field accelerators in general, in fact) is outlined in the next section. And lastly, probably most critically, electron beam-based wake-field accelerators are easily phase-locked, in the sense that when one uses a the same rf wave and compressor to create both the drive beam and witness beam, both beams will tend to be locked to the rf clock. This point is elaborated upon further in Section IV.

2.2 STAGED PWFA — A COLLIDER MODEL

Given the promise that the nonlinear PWFA shows in terms of both preservation of beam quality and achieving high gradient acceleration at moderately short wavelength, it is reasonable to ask whether this type of acceleration mechanism is appropriate for high energy physics colliders. We will therefore consider in this section a "straw-man" design for a collider based on the nonlinear PWFA. This exercise will point out the issues that must be addressed in a proof-of-principle staging experiment.

One limitation of this technique for creating an electron-positron collider is apparent from the beginning - that positrons are not easily accelerated using in this type of plasma wave. Therefore one is by definition considering alternative schemes such as e-e, e-γ or γ-γ colliders. We will therefore present the design from the accelerator point of view, leaving the details of the interaction region purposely vague.

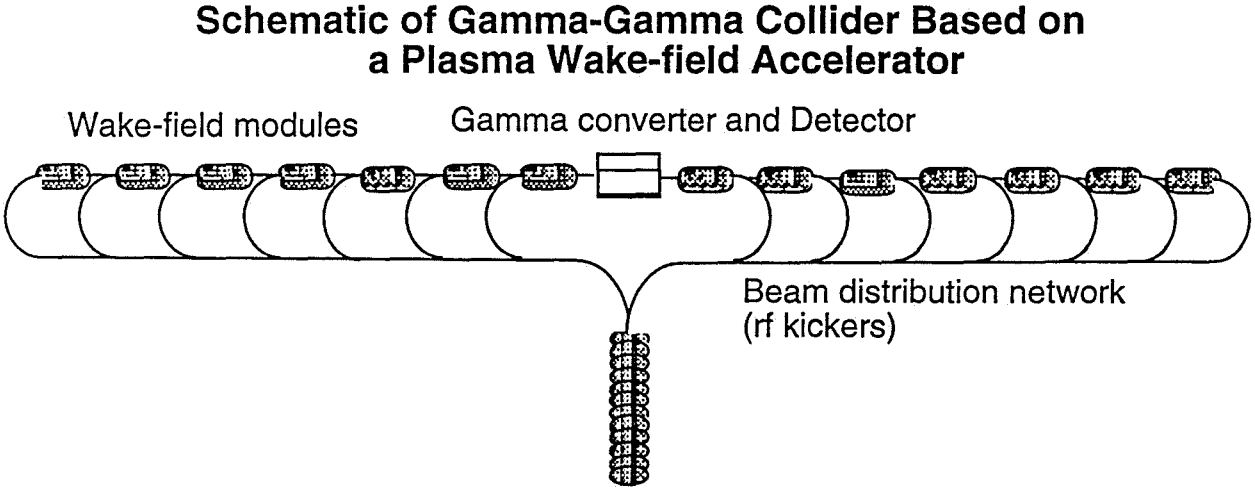

Figure 7. Schematic of a γ–γ collider using a hardware transformer scheme. A large number of bunches are created in heavily beam-loaded linac fed by an rf photoinjector based on a compressor. Separate wake modules are driven by the beams, which are fanned out in a binary rf splitting scheme.

It was originally pointed out by W. Gai[7] that one could mitigate concerns about the transformer ratio of wake-field accelerators by driving a large number of wake-field modules from one work-horse linac. A schematic of a variation on this "hardware transformer" is shown in Figure 7. The single linac which feeds both sides of the collider must then have as many bunches in a single rf fill as the total number of modules, and in this geometry, they must be separated by the time-of-flight through a single module section, including drift. This heavily beam-loaded linac is fed by an rf photoinjector employing one or more magnetic compressors. The separate wake modules are driven by the beams, which are fanned out in a binary rf splitting scheme which is driven at the half-sub-harmonic of the linac rf frequency. These drive bunches must also be combined with the accelerating bunch, which because it will be over a TeV in energy at peak, must not see bend fields or they will radiate large amounts of energy through synchrotron photons. Thus the recombining sections must also be based on (very high frequency ~ 50 GHz) rf kickers. The stability of these rf splitting and combining systems is of course critical in determining the performance of the collider.

The first quantitative step in constructing this straw-man design is to self-consistently determine the length of a module, by setting the decelerating gradient of the beam in the module, and the energy of the beam exiting the drive linac. The decelerating gradient is of course dependent on the beam charge, emittance, bunch length and plasma density. These parameters are determined by simulation of the plasma wake-field interaction (detailed simulations with similar parameter sets are given in a following section), and are given in Table 1. Once the decelerating gradient is chosen, the accelerating gradient and plasma wavelength are also known; it remains to choose the length of the module, which sets the linac energy, as we will take the length of the module to be such that the trailing edge of the drive beam loses 95% of its energy in the plasma. The energy in turn is chosen partially by geometric considerations and partially by beam-loading considerations, the results of which are displayed in Table 2. Note that the stored energy

per pulse is quite large (60 J). This compares quite favorably with laser sources of similar repetition rates.

The length of the intermodule drift in the collider is chosen to give sufficient space to bring in a new drive beam and remove the spent one, match the accelerating beam optics from one module to the next, but keeping the dead (non-accelerating) space to a minimum. The total accelerating module plus dead space length is finally chosen to be commensurate with a subharmonic of the drive linac rf wavelength.

Beam Energy	3 GeV
Beam Charge	20 nC
Stored Energy/Bunch	60 J
Bunch Length (compr.)	0.8 mm
Norm. Emittance	50 mm-mrad
Plasma Density	2×10^{14} cm^{-3}
Plasma Wavelength	2.2 mm
Deceleration Wake	500 MeV/m
Accelerating Wake	1 GeV/m
Length of Wake Module	5.7 m
Length of Intermodule Drift	2.66 m

Table 1. Nominal drive beam and accelerating module parameters for the plasma wake-field accelerator-based collider shown in Figure 7.

Table 2 shows a set of design parameters for the heavily beam-loaded drive linac based on a normal conducting TESLA-like 1300 MHz structure; by heavily beam-loaded, we mean that the beam power is well in excess of dissipated rf power. The accelerating gradient is chosen to be relatively low (6 MeV/m), in order to mitigate the rf power dissipation and related issues. These issues in this case include the peak and average power per cavity at the chosen 5% duty cycle; the peak power of 5.9 MW at a pulse length of 14.5 μsec (78% of this power goes into accelerating the drive bunches) is easily achievable. The nominal average dissipated rf power is 66 kW, which is a similar power to the TTF photoinjector power, but with nearly an order of magnitude more total mass. The cooling of this cavity should therefore be a straightforward design problem.

Avg. accelerating gradient	6 MeV/m
Shunt impedance ZT^2	30 MΩ/m
Active length	500 m
Cavity length	1.1 m
Peak rf power supplied to cavity	5.9 MW
Number of bunches	2 x 250
Beam current (in fill)	690 mA
RF flat top	14.5 μsec
Duty cycle	5%
Avg. bunch production rate	865 kHz
Diss. rf power/cavity (avg.)	66 kW
Total ave. diss. RF power	30 MW
Total avg. beam power	104 MW

Table 2. Design parameters of heavily beam-loaded 1300 MHz drive linac for plasma wake-field collider. Parameters chosen based on Table 1 parameters, optimized for high level of beam-loading (beam power well in excess of dissipated rf power).

Table 3 shows the parameters associated with the accelerated beam and the total system performance. The efficiency of energy extraction from the wake is kept to 20%, in order to load the beam at 91% of the peak amplitude (transformer ratio of approximately 1.8 per module). This gives a center-of-mass energy at the collision point of 2.5 TeV, with collisions occurring at an average rate of 3.5 kHz. Assuming a wall-plug efficiency associated with the 1300 MHz rf system of 40%, we obtain an average power of 335 MW to run the collider. This is within the range of acceptable powers for this type of third-generation (post-NLC) collider.

Accelerated charge	2 nC
Wake efficiency	20%
Length of Collider	2 x 2.16 km
Accel. beam energy	1.25 TeV (beam loaded)
Avg. collision rate	3.5 kHz
Drive linac/wall effic.	40%
Total wall power (drive)	335 MW
Total efficiency	7.6%

Table 3. Accelerated beam and the total system performance of collider.

No luminosity estimates will be attempted at this point, as there are many issues associated with the emittance dynamics in the collider, as well as the detailed design of the ($\gamma-\gamma$, $e^-\gamma$ or e^--e^-) collider final focus and interaction point. The interaction point is a complex subject well beyond the scope of present consideration; let us examine the issue of emittance momentarily.

There are two fundamental physical mechanisms which give rise to emittance variation in this type of accelerator - emittance damping due to dipole radiative decay of the betatron oscillation amplitude, and emittance growth due to multiple scattering off of the plasma ions. Of course, there are many other sources of emittance growth, including higher focusing multipole moments, chromatic and collective transverse instability.

The damping of oscillations in a uniform focusing channel such as the plasma ion-focusing column we are considering has been analyzed in detail by Huang, Chen and Ruth[8]. The equation for emittance damping derivable from this work is

$$\frac{d\varepsilon_n^2}{dz} = -\frac{2\pi r_e^2 n_0}{3}\varepsilon_n^2, \tag{2.6}$$

which yields exponential damping with characteristic length $z_d = 3/2\pi r_e^2 n_0$. For the plasma densities of interest here this damping length is enormous, on the order of 10^8 m, and thus we can ignore this effect henceforth; only in the case of a nearly solid state plasma density would this effect be strong enough to consider.

On the other hand, the excitation of the emittance growth due to multiple scattering can be quantified by the following expression, based on the familiar angular growth formula due to Bethe,

$$\frac{d\varepsilon_n^2}{dz} \cong 9.13\left(\frac{n_0 r_e^3}{\gamma}\right)^{1/2}\frac{Z^2\ln\left(184/Z^{1/3}\right)}{A}\varepsilon_n. \tag{2.7}$$

Equation 2.7 can be integrated, under the assumption of small emittance growth, to give

$$\Delta\varepsilon_n^2 \cong 18.25\left(n_0 r_e^3 \gamma_f\right)^{1/2} \frac{Z^2 \ln\left(184/Z^{1/3}\right)}{A} \frac{\varepsilon_n m_e c^2}{eE_{acc}}. \tag{2.8}$$

For the parameters of this collider design the rms normalized emittance increase, assuming a hydrogen plasma and beginning with an rms normalized emittance of $\varepsilon_n = 10^{-8}$ m-rad (the vertical emittance from a state of the art damping ring), is $\sqrt{\Delta\varepsilon_n^2} \cong 1.33 \times 10^{-9}$ m-rad, consistent with the assumption of small growth.

It should be noted at this point that the laser-driven variations on plasma acceleration, *e.g.* laser wake-field acceleration, generally demand a higher plasma density in order to guide the laser in analogy to the ion-focusing considered here. This is because the effective emittance of the laser beam is proportional to the photon wavelength, $\varepsilon_l = \lambda_l / 4\pi$. Thus for the infrared lasers used to create the picosecond terawatt pulses needed to drive the laser wake-field in plasma, the effective transverse emittance is orders of magnitude larger than the multi-GeV electron beam we have considered in our design. The laser divergence must be controlled by a strongly focusing channel, which implies a high density[9]. Thus, unless a completely evacuated channel is used[10], the multiple scattering driven emittance growth will be a larger, perhaps non-negligible issue for laser-plasma accelerators.

As a final comment on the subject of emittance growth, we note that in our collider design, the drive beam and the high energy accelerating beam must be brought together on a collinear path without bending the accelerating beam. This is because, even with the much smaller bend angle experienced by the high energy beam, it will radiate prohibitively high energies of synchrotron photons at an electron energy in the TeV range. Thus we must consider a high-frequency kicker system (similar to that which is developed at low frequency for the FTF experiments, see discussion in Section IV) to avoid bending the

accelerating beam. This complication can be avoided in principle by using an annular laser wake-field driver.

III. REVIEW OF THE UCLA/ARGONNE EXPERIMENT

3.1 PLASMA AND BEAMLINE OVERVIEW

A hollow cathode arc plasma source has been installed at the end of the Argonne Wake-field Accelerator (AWA), with its associated vacuum equipment and diagnostics, and is shown schematically in Figure 8. The plasma has been characterized completely in the last two years, by use of electrostatic probes and a 140 GHz microwave interferometry system whose components were partially obtained from the University of Wisconsin Plasma Physics group. The plasma was found to have a very uniform interelectrode (tantalum cathode, steel anode) longitudinal density profile (<20% variation) with densities tunable between 5×10^{12} and 10^{14}/cc. These data (see *e.g.* Figure 9) were taken with the electrostatic probes, which were calibrated by use of the interferometer. The density uniformity is critical, because a large variation in this quantity produces large changes in the frequency (and therefore the phase seen by a trailing beam) of the wake-field.

Because of the demands of matching the beam into the strong transverse focusing of the plasma, and to avoid depleting the electron beam energy in the hoped for high gradient cases, the plasma column has been tailored to be short (<10 cm), with fairly large angular acceptance of the anode and cathode "beam tubes". A differential pumping system has been implemented which uses two turbomolecular pumps to obtain a vacuum pressure measured to be 1.5×10^{-7} Torr at the end of the AWA linac. The large solenoid (25 cm in length, B>0.5 T) used for focusing and matching the beam into the plasma has been constructed and implemented. In order to match correctly into the plasma, we have used the measurement of the plasma density profile in the upstream (cathode) region to generate the correct profile of the ion focusing.

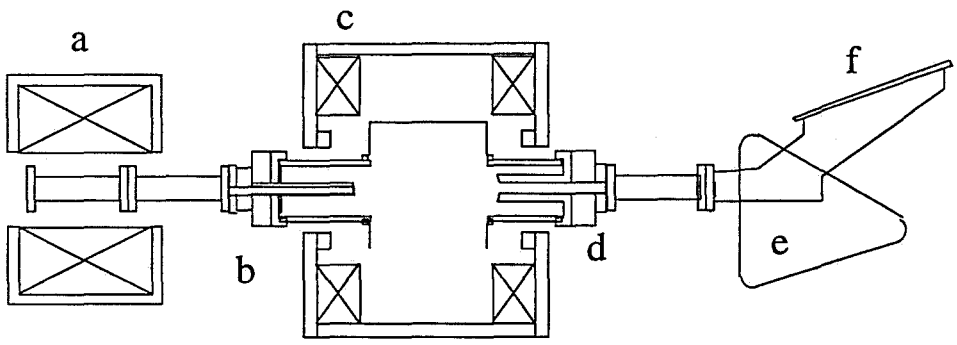

Figure 8. Plasma experimental layout: (a) matching solenoid, (b) improved acceptance cathode assembly, (c) plasma vessel with confinement solenoid, (d) anode assembly, (e) 60 degree dipole spectrometer and (f) focal plane.

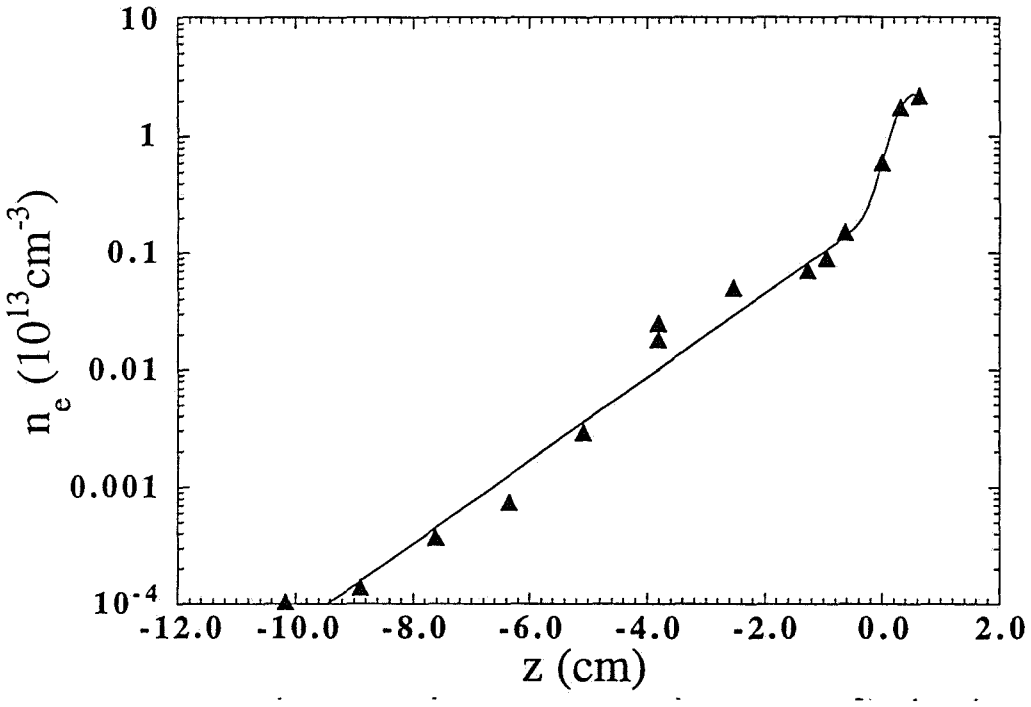

Figure 9. Electron beam density within the cathode region of hollow cathode arc plasma.

A further plasma diagnostic has been developed to measure x-ray emission from the hot plasma which develops after the coherent wake wave dissipates into turbulent motion. The ions emit VUV to soft x-ray radiation which has been proposed by Los Alamos to be a

useful debris-free (as opposed to laser-target) sources for x-ray lithography. We have added to the plasma vessel a VUV monochromator, as shown in Figure 8, to measure the spectrum of emitted radiation. An Ar+ ion line at 120 nm is expected to be most prominent for our experimental conditions. As the theoretical understanding of the energy transfer processes in the turbulent, nonequilibrium plasma is only crude at this point, this diagnostic is only qualitative at this point. The relatively primitive state of the theoretical model is partially due to the difficulty of dealing with a large number of atomic transitions, but also due to some restrictive assumptions concerning the distribution functions in the plasma. We are now looking into improved modeling of these processes using electron distribution functions derived from PIC codes.

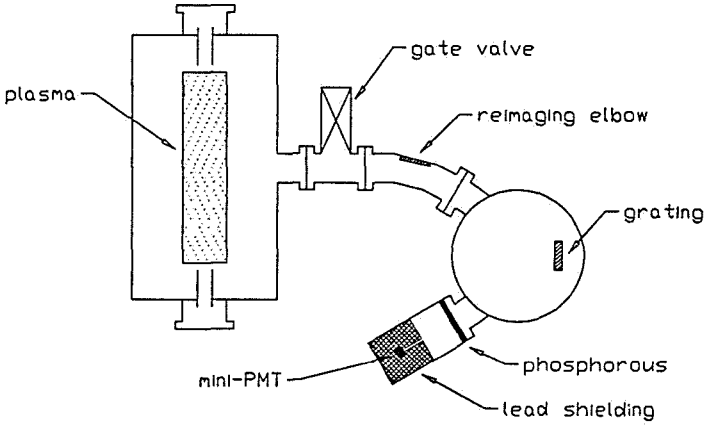

Figure 10. Schematic of the experimental setup for VUV plasma emission measurements.

We have developed our beam diagnostics in collaboration with the Argonne group. The bulk of the beam energy spectrum at the exit of the plasma is measured with a phosphor screen/video system after a 60 degree bend in a dipole magnetic spectrometer. The high energy tail is to be characterized by use of a 16 channel hodoscope obtained from

the Argonne HEP equipment pool. This diagnostic has been in fact installed and recently was found to work satisfactorily when well shielded against bremsstrahlung x-rays from the AWA. Emittance has presently been measured by the AWA group using a pepper pot, with the UCLA slit-based system to be installed shortly as an integral part of the plasma experiment. Beam charge is measured with Faraday cups and shot-by-shot by non-destructive integrating current transformers (ICTs).

Bunch length measurements using the streak camera have been based on Cerenkov radiation derived from thin quartz plates, with examples of these streak images given below. More refined streak camera-based methods based on use of Aerogel are under development.

3.2 Experimental Measurements of Plasma Wake-fields

Initial measurements, performed in December 1994 and April 1995 , attempted to concentrate on establishing only the following characteristics of the blow-out regime of the plasma wake-field accelerator: beam energy loss and acceleration. The observation of acceleration requires that a weak "witness" beam be placed with a small delay (<2 cm) behind the center of the driving bunch. We have used the AWA multiple-ring reflector system (pulse-shaper) for the photocathode drive laser which delays a small core of the laser pulse by the appropriate amount to generate this witness beam, as shown in the current profile obtained from a streak camera image found in Fig. 11. This is a very robust way of producing a (space-charge dominated) witness beam with similar propagation characteristics to the drive beam, because its density and thus its beam plasma frequency must be very nearly the same. If the beam plasma frequencies of the drive and witness beams are very different, it would not be possible to simultaneously propagate both of them to the experimental area.

While we have, we believe, experimentally barely accessed the blow-out regime in our initial measurements of bunch length and transverse size, the preliminary results of the experiments give acceleration gradients nearly two orders of magnitude smaller than our ultimate design goal. Before discussing the energy measurements explicitly, we first explain this shortfall. While some of the problem lies with charge (we have transported less than 20 nC to the plasma in the drive beam) a more important factor is bunch length. Another aspect of the current profile apparent from Fig. 11 is that the length of the drive pulse is about 24 psec FWHM, which is over three times the length assumed in the optimized case of Fig. 6. Because the wave-number of the driven plasma wave must satisfy $k \cong k_p \leq 2/\sigma_z$, in order to drive the highest amplitude waves, this implies that we must lower the plasma density by one order of magnitude. Now, the PWFA can be looked at as the Cerenkov emission of plasmons, and the (initial) presence of plasma electrons in direct contact with the beam guarantees that plasma wake-fields have in fact the maximal coupling over beam charge to emitted field that the Cerenkov mechanism allows. The wake-field behind the beam in the PWFA can therefore be estimated to be[11]

$$|eE_z| \cong N_b e^2 k_p^2 = 4\pi n_0 N_b r_e^2 m_e c^2 \leq \frac{4N_b e^2}{\sigma_z^2}. \tag{3.1}$$

Thus the maximum wake-field depends quadratically on the inverse of the bunch length (or equivalently, the maximum allowed plasma density for that bunch length), and a great premium is placed on shortening the bunch length. Given that both the number of particles per bunch was smaller by over five, and the inverse of the bunch length was smaller than the original proposal by an order of magnitude, it is not surprising that relatively small accelerating gradients were measured.

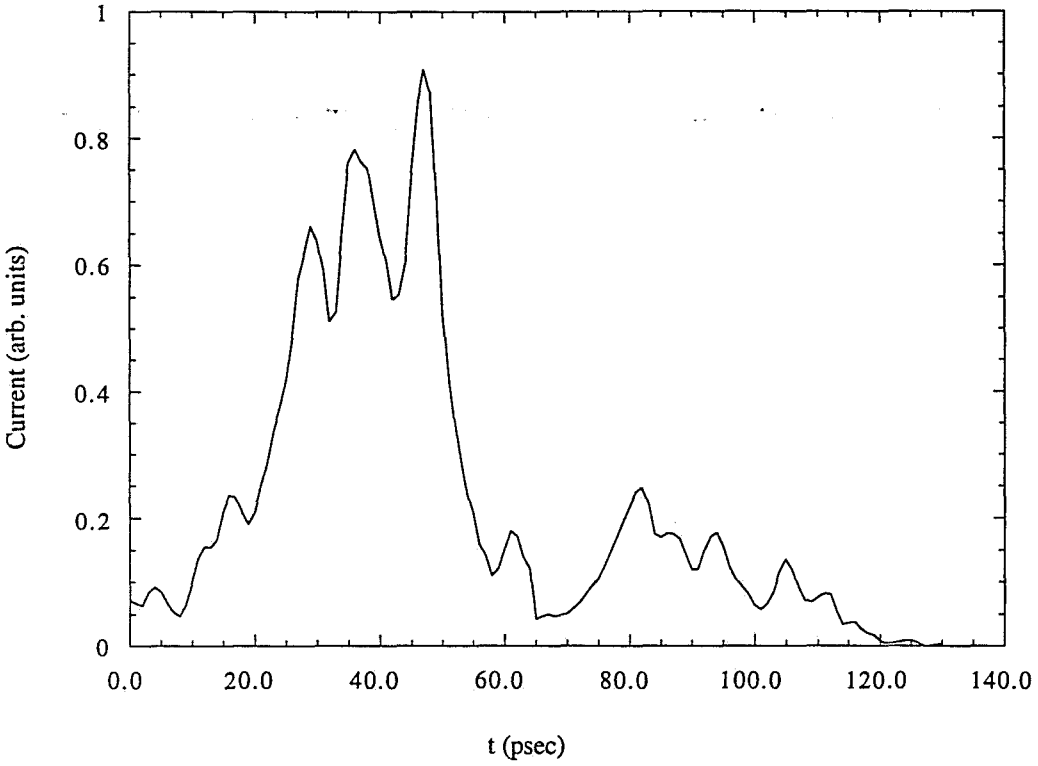

Figure 11. Streak camera image of beam current profile from AWA during plasma experimentation, showing drive beam of approximately 15 nC and witness beam of about 3 nC.

With our witness beam setup in the AWA, it is not possible to separate the witness and drive beam energy spectra in the magnetic spectrometer image plane. Thus, when the witness beam accelerates, we have a large uncertainty in the acceleration gradient because we do not know the initial energy of the witness pulse - we can only set a lower bound on the gradient. Because the wake-fields and the space charge in the rf photoinjector are decelerating for the witness beam, for the small accelerations we have measured this is a relatively large effect.

Representative data for the last run up until this writing are shown in Fig. 12, which displays the upper end of the energy spectrum as measured by video camera capture of a scintillating plate. The presence of the witness beam is not noticeable until the plasma is on, then an accelerated tail is generated. With no witness beam, the high energy tail is

decelerated, as could be expected. The data indicate an average acceleration in the extreme tail of 9 MeV/m, which is nearly as well as was done in the original PWFA experiments[12] at the Argonne Accelerator Test Facility (AATF). This again may be underestimated due to the uncertainty of the witness beam energy spectrum before the plasma. Calculations using the fluid code indicate a slightly larger gradient, in the range of 12-20 MeV/m. The maximum energy gained by the tail of the distribution could have been clarified by a more sensitive diagnostic, such as the hodoscope. This type of diagnostic was not, due to noise problems, used on the first round of experiments. Since these problems are now controlled, such a measurement will be available for the next tests.

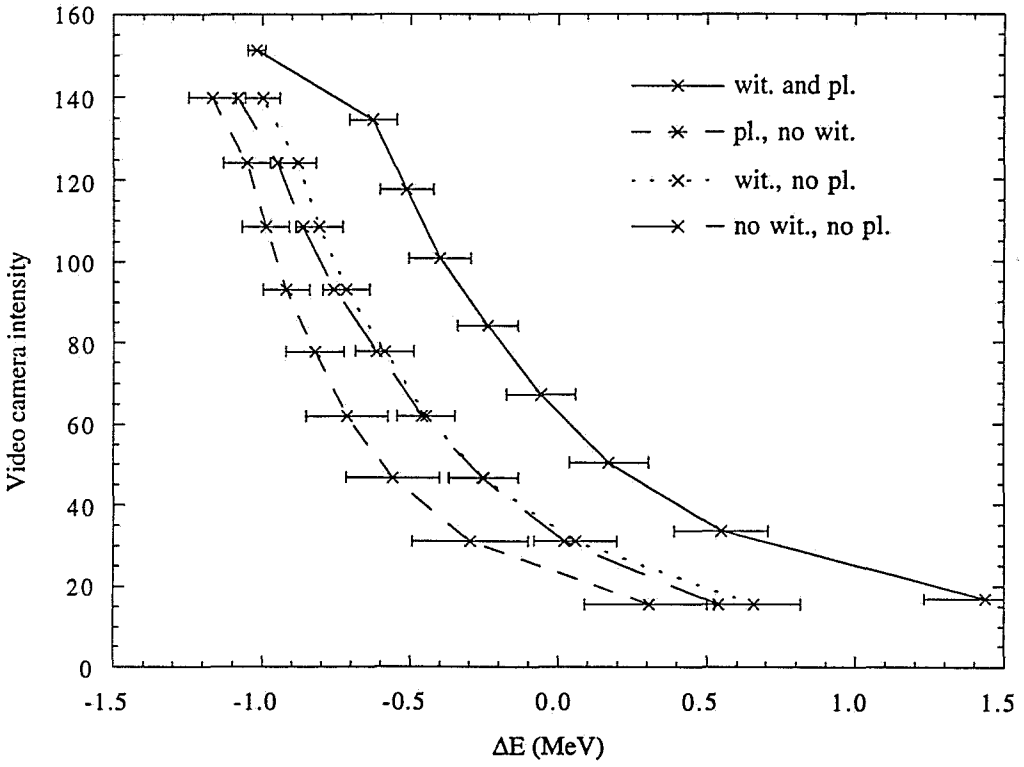

Figure 12. Observation of the high energy tail at spectrometer. In the legend, wit. indicates witness beam and pl. indicates plasma present.

In addition to the observation of drive beam deceleration and wake-field acceleration, experiments have been performed to diagnose the self-focusing and transport of the drive beam in the plasma. Although the initial wake-field acceleration experiments

demonstrated that an accelerating wake-field was excited, the fact that its magnitude was not larger suggested that the best place to look for an improvement is to examine the propagation of the drive beam, especially because effective propagation relies on a self-focusing effect. Given the wake-field data, as well as the general characteristics of the beam as diagnosed in separate AWA measurements, the beam parameters are near the border of being able to bring about and maintain a complete rarefaction of the plasma electrons for the duration of the beam transport in the plasma. This served as motivation for performing a separate experiment to examine these issues in more detail. Additional motivation came from the fact that previous focusing experiments have used either long beams or low beam densities, with no data for short ($<\lambda_p$), underdense beams. The focusing experiment, therefore, is an opportunity to check the theoretical understanding of drive beam matching, focusing and equilibration, and also to test precisely how well this works in our case.

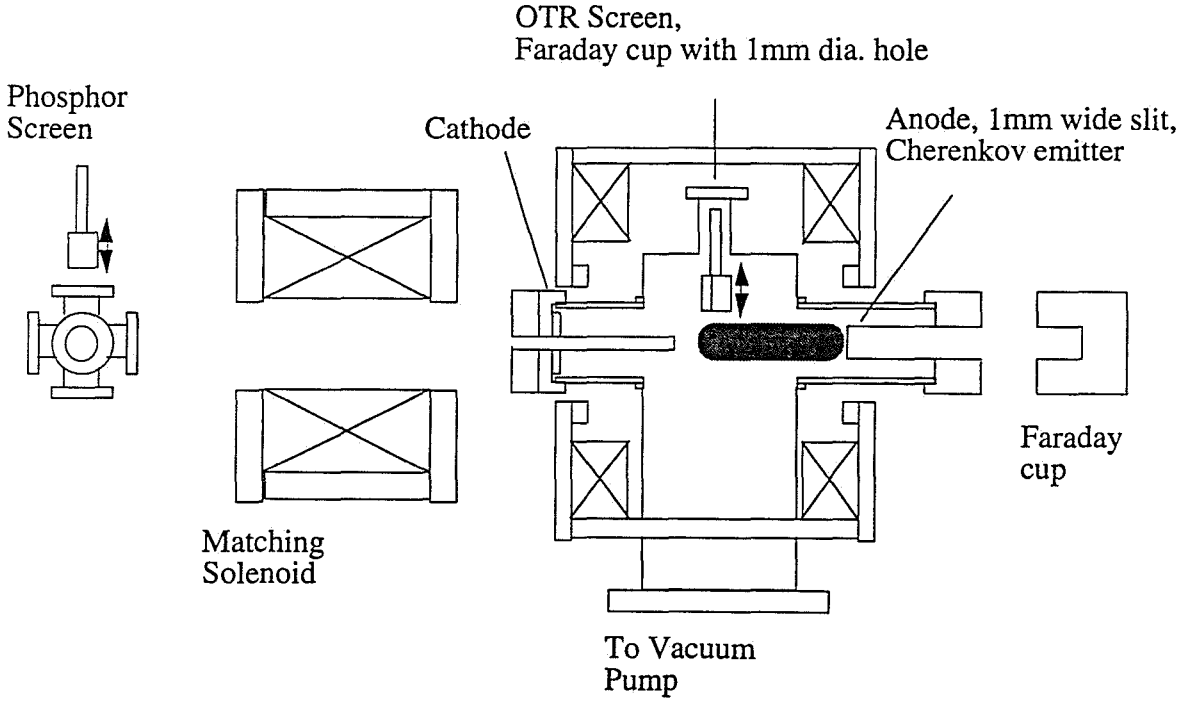

Figure 13. The experimental configuration for underdense beam propagation in plasma measurements.

The layout for the focusing experiment is shown in Fig. 13. The incoming beam is measured at the waist after the solenoid to determine its peak density, radial profile and (in future runs) temporal structure. An OTR screen and CCD camera measure the radial profile, after which the beam is steered through a 1 mm dia. hole to measure the charge transmitted. The peak density is then computed, conbining the hole transmission and the radial profile data. The measurements at the waist, and the image from the phosphor screen before the solenoid can give an estimate for the emittance. An additional method for computing the emittance is with a solenoid scan: the solenoid current is varied and the beam spot sizes at the OTR screen are fitted to a beam envelope model. To verify that the accelerator parameters have not drifted during plasma operation, the measurements of the initial focus are performed both before and after the plasma arc has been on.

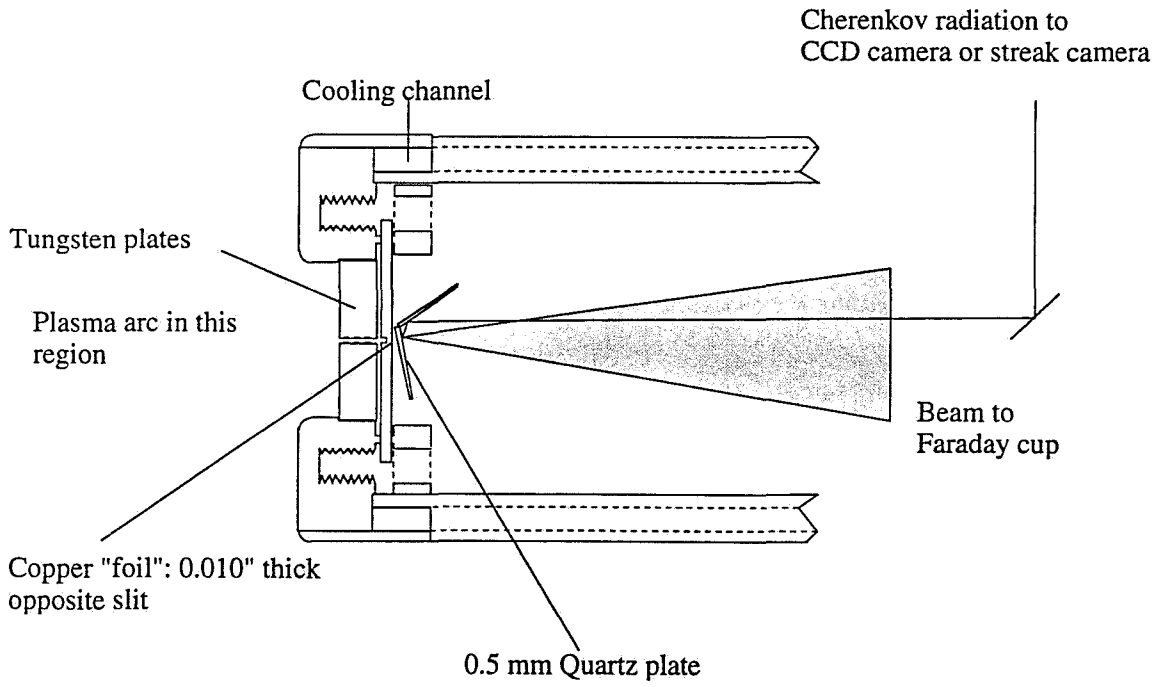

Figure 14. Plasma anode (downstream end) diagnostics for underdense beam propagation in plasma measurements.

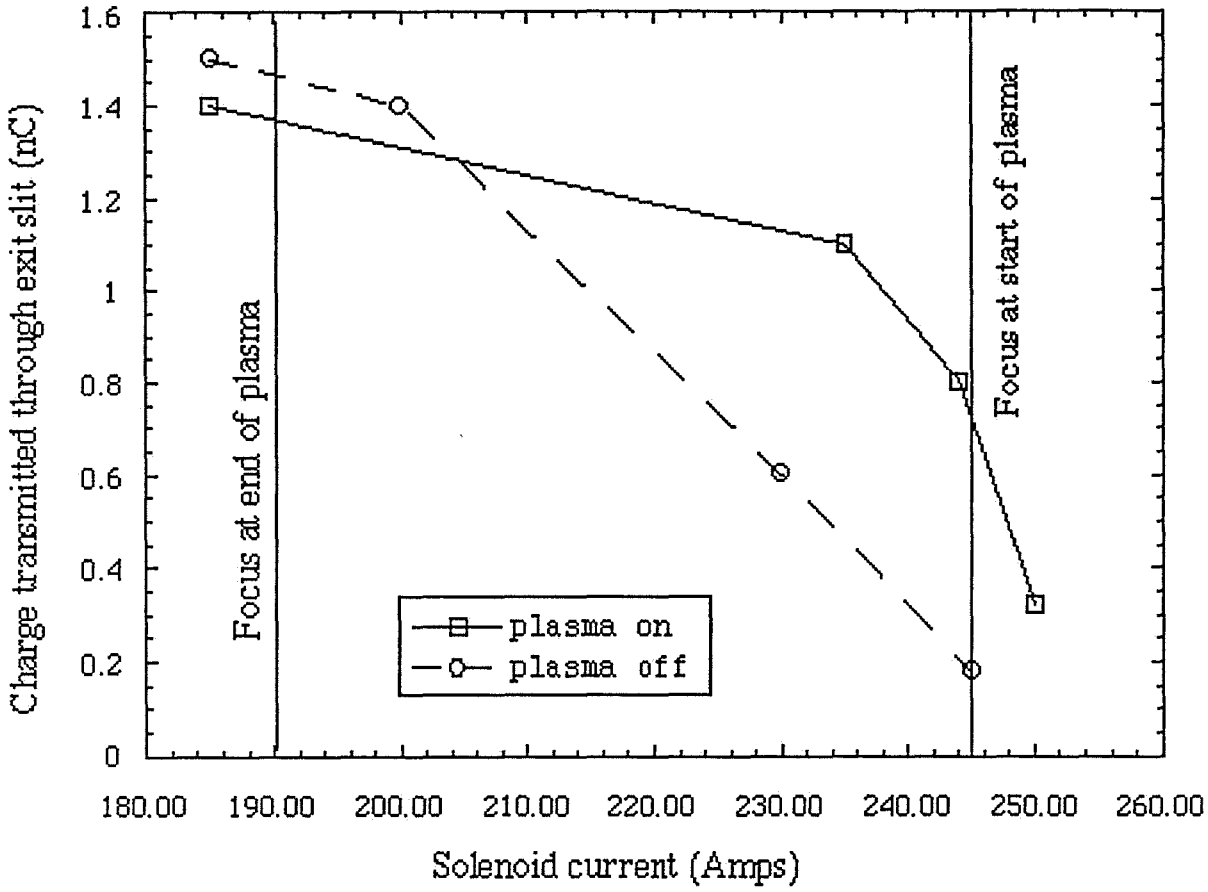

Figure 15. Charge transmitted through anode plate in plasma focusing run.

With the plasma off and the waist at the OTR screen, the beam simply drifts for 10 cm before reaching the diagnostics contained in the anode, shown in Fig. 14. Here, the beam is collimated with a 1 mm wide slit. The charge that passes through this slit is registered in a Faraday cup, usually a very small number when the beam is allowed to drift in the absence of plasma. The transverse profile after the slit is also measured with a Cerenkov emitter and CCD camera. This image is much larger transversely than the original waist in the case of a freely expanding beam. In the future, this profile will be measured with picosecond time resolution using a streak camera, a technique used on overdense plasma focusing experiments at Argonne.

The same measurements are performed with the anode diagnostics when the plasma is turned on. As expected the charge transmitted through the 1 mm slit increases and the profile at the Cerenkov emitter becomes peaked and narrow. Fig. 15 is an example of the type of data taken with this experimental configuration setup. The initial beam waist does not need to remain at the beginning of the plasma column, and so the solenoid current is varied, effectively changing the propagation distance of the beam in the plasma. When the solenoid is turned down, the beam remains large in radius through most of the plasma column, giving results very much like the plasma-off case. As the solenoid is turned up in strength, the transmission through the slit degrades very slowly, with rapid variations when the waist is swept past the start of the plasma column, which affects the matching of the beam into the focusing channel.

The focusing experiment has had a total of five experimental runs. The aim for future runs is to achieve a greater amount of repeatability for this experiment, through a more thorough and systematic measurement of the initial conditions. Our experience with this experiment suggests that, given the AWA beam, we may not be able to maintain the underdense regime throughout the propagation distance. To achieve this state, calculations indicate that it may be necessary, for example, to have about 70 % more charge, keeping all other parameters constant.

3.3 CONCLUSIONS

In summary, the experiments at Argonne[13] were a mixture of success and disappointment. The reasons for the experiments at the AWA falling short of expectations are clear from the previous discussion:

- The beam charge was smaller than expected by a factor of five.
- The ratio of the emittance to the charge was found to be larger by a factor of 2.5. This limited the total charge that could pass through the cathode aperture, and made us work at the edge of violating the minimum requirement for blowout of the plasma electrons.
- The bunch length was a factor of three larger than expected, producing a very large effect - the expected wake-field is smaller by one order of magnitude.

The experiments produced a number of useful results which give us confidence to move forward to the next step:

- Longitudinal wake-fields were produced in fairly good agreement with the computational models.
- These fields were measured by a new and unique method of producing a witness beam using a delayed section of the photocathode laser pulse.
- Experiments showing the transverse focusing and transport of the beam were performed at or just beyond the boundary of the underdense regime where the drive beam is well guided and the plasma electrons are completely rarefied.

It could be observed that many of the shortfalls associated with bringing this experiment up to the GeV/m level in the blowout regime could be solved by shortening the bunch length. This could be accomplished using a magnetic compression system in

principle, but this is problematic within the context of the AWA. To begin, the system is designed for maximum charge output with minimum energy spread, without regard for emittance. This implies the beam must remain large in the low shunt impedance (therefore low beam impedance) linac sections, or longitudinal space charge produces large energy spread and debunching of the beam. This is unfavorable from the point of view of emittance (one obtains approximately 10-15 mm-mrad/nC normalized emittance, as opposed to 1-2 mm-mrad/nC for optimized emittance compensated photoinjectors), and not terribly effective at preserving the longitudinal phase space as well. One can in principle compress a 20 nC pulse to 1 mm rms bunch length, but not a 50 nC pulse, and only by running very far off crest in the linac sections, which only supply about 12.5 MeV acceleration after the 2.2 MeV gun when run on crest - to run 30 degrees of crest implies a final energy of only 13 MeV. In addition, this 20 nC pulse is expected to have a normalized emittance of over 200 mm-mrad, which implies a reduced level of wake-field driving effectiveness.

Because of all of these factors, we have decided that the next step is much more likely to be successful using the compressed beams available at the FTF. The FTF photoinjector is identical in design to the TESLA Test Facility (TTF) photoinjector, and is optimized to produce a low emittance (space-charge compensated), high charge, compressible beam. The design of this system, as well as the physics and engineering issues of pulse compression, are discussed further below.

IV. NONLINEAR PWFA EXPERIMENT AT THE FTF

4.1 THE FTF PHOTOINJECTOR AND COMPRESSOR

The FTF is an rf photoinjector facility being constructed at Fermilab, as a collaboration between Fermilab, UCLA, INFN-Milano, and the University of Rochester, and is designed to test the design principles of the TESLA Test Facility (TTF) photoinjector before the installation of the device at DESY in late 1997. These principles include the self-compensation of the space charge-induced emittance, compression of an ultra-high current beam without emittance dilution, handling of high average power load in the rf gun, and operation of a photoinjector with a superconducting booster linac. The FTF is also under consideration as a host research facility for experimentation on high-brightness, short-pulse beams; candidate experiments include this proposal, as well Compton scattering experiments promoted by the Rochester group.

Because the FTF test agenda is so ambitious in its modeling of the TTF photoinjector performance, for most of our purposes the facility can be thought of as a copy of the TTF injector. As this injector has been studied quite thoroughly in the design phase, it is straightforward for us to use design tools to adapt the FTF photoinjector design to the needs of this experiment.

The FTF photoinjector is shown in Figure 16, which displays the layout as it is planned for the A0 laboratory at Fermilab. The photoinjector lies inside of a shielding bunker, with a nearby laser facility to provide the photocathode excitation pulse as well as larger energy pulses for Compton scattering experiments. The photoinjector consists of a ultra-high average power (65 kW at 10 Hz repetition rate) rf gun, a superconducting TESLA cavity used as a booster linac, and chicane compressor to yield sub-mm rms pulse

lengths. The expected performance of this device for TESLA parameters has been the subject of intensive design studies[14]; the characteristics of the injector for these parameters are summarized in Table 4.1.

In the course of studying the physics of rf photoinjector design, we have developed a very powerful technique for scaling designs in both bunch charge and rf wavelength[15]. Using this technique, we have, for instance, generated a very low emittance, low charge design suitable for FEL injection at 1300 MHz[16], from a 2856 MHz design, and an ultra-low charge (30 pC), ultra-short compressed bunch (42 μm) design from a 1 nC, low-emittance design[15]. For present interest, we have used charge scaling in the TTF design to extend the design to 20 nC, as is used in the collider design discussed above. The results of PARMELA simulation of this parameter set is shown in Figure 17. It should be emphasized that to obtain these beam parameters, one must only change the characteristics of the laser on the cathode and the settings of the focusing solenoids. *No hardware changes are necessary* from the basic FTF layout..

Beam Charge	20 nC
Beam Energy	18.6 MeV
Norm. Emittance (after compression)	80 mm-mrad
Bunch Length (after compression)	0.8 mm

Table 4.1. Beam parameters for high charge FTF photoinjector case, for plasma wake-field acceleration experiments, derived from PARMELA simulation.

It should be noted that these beam parameters are somewhat different from the collider design, mainly in the low beam energy (18 MeV), which impacts the trace space emittance. It is quite probable, however, that the normalized emittance achieved in the FTF design will not be much smaller than seen in these simulations, as this lower bound is set by the performance of the emittance compensation system at low energy.

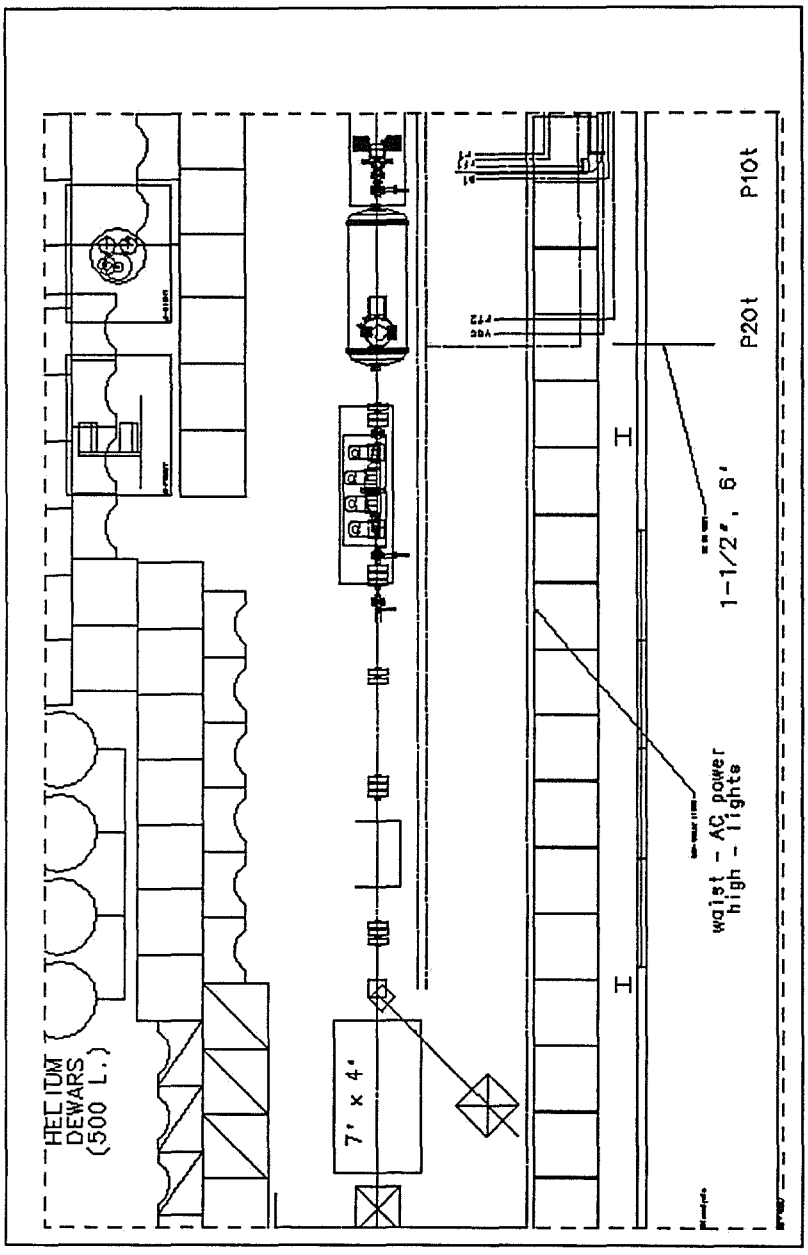

Figure 16. Layout of the rf photoinjector in the Fermilab Test Facility, showing rf gun, superconducting booster linac, and chicane compressor.

(a)

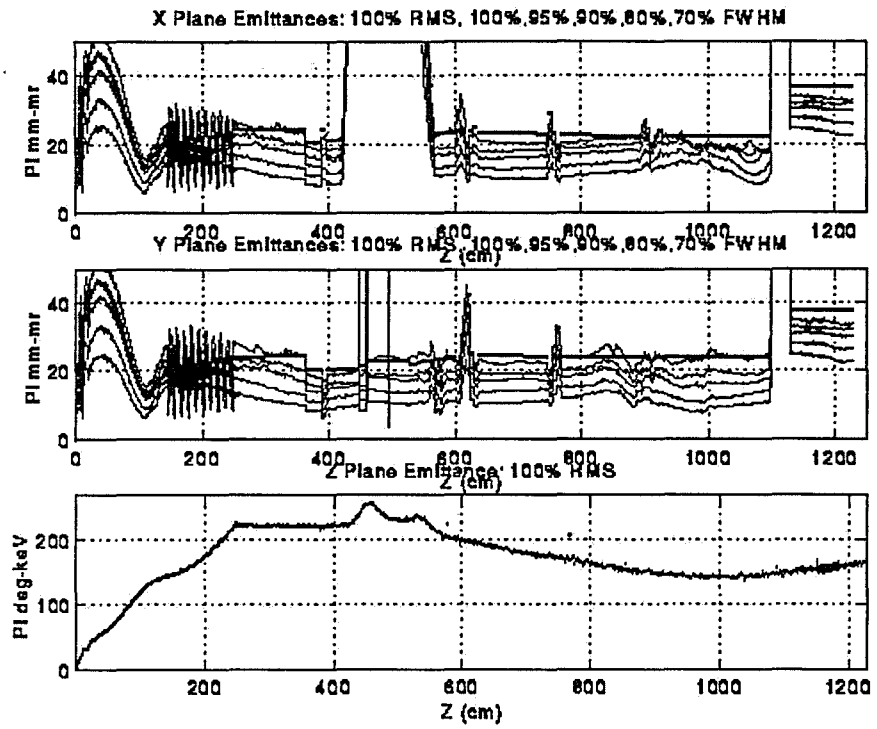

(b)

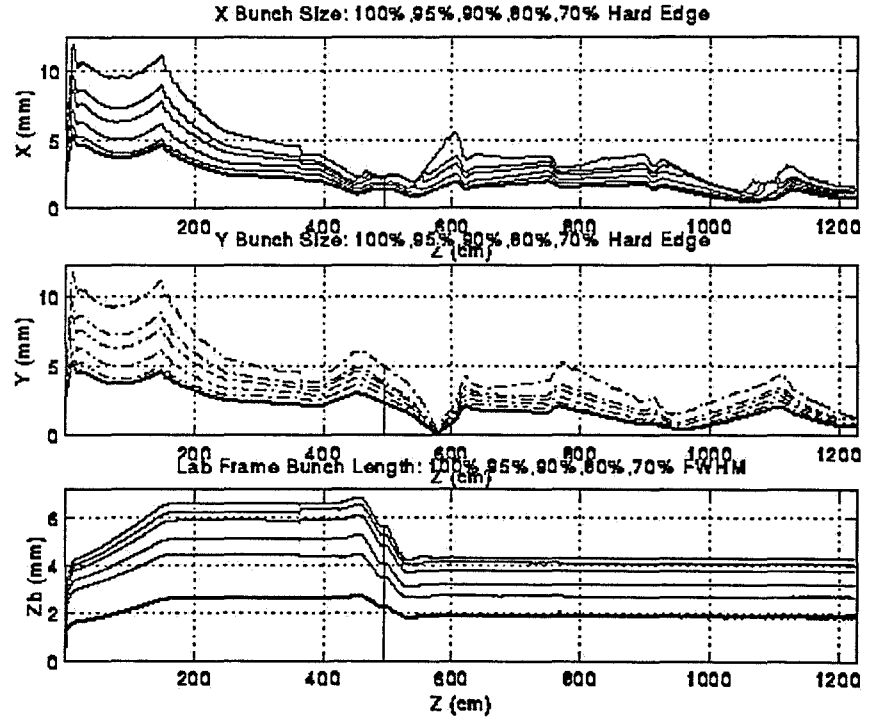

Figure 17. Beam equivalent FWHM (a) emittance and (b) envelope evolution through photoinjector, compressor, and matching solenoid, in high charge FTF case.

4.2 EXPECTED PLASMA WAKE-FIELD PERFORMANCE

For the type of beam extractable from the FTF photoinjector, we have calculated the expected performance of the FTF high charge beam as a wake-field driver, using the particle phase space derived from PARMELA as input to a particle-in-cell code developed at UCLA. Results of this calculation, in which the beam is matched to the focusing of a $n_0 = 10^{14}\text{cm}^{-3}$ plasma, are shown in Figure 18.

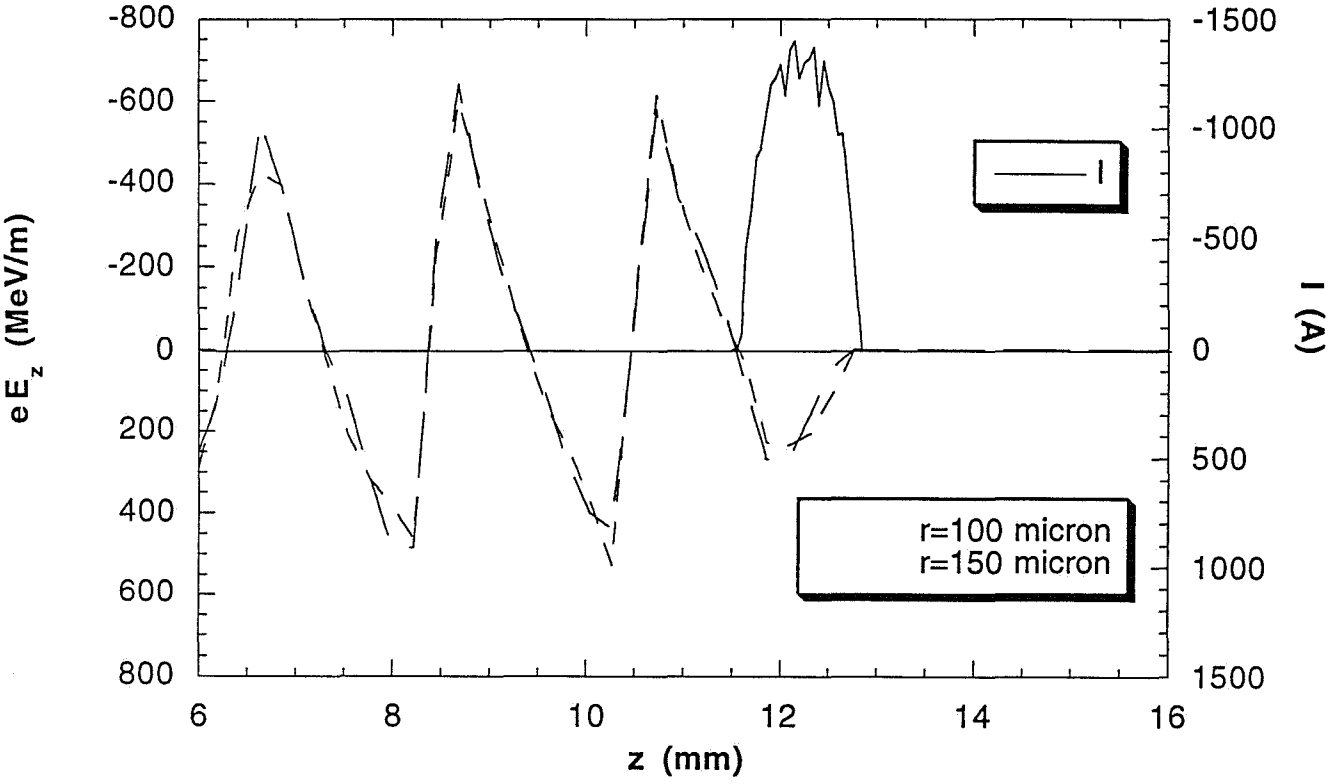

Figure 18. Beam current and longitudinal wakes at two radii offset from the axis, displaying blow-out in a $n_0 = 10^{14}\text{cm}^{-3}$ plasma.

The plasma density is chosen a factor of two lower than optimum for maximizing longitudinal wakes. This is to ease the focusing requirements (chromatic effects in the matching solenoid blow up the transverse emittance, *cf.* Fig. 15(a)), and to lower the

decelerating gradient. With this lower gradient the plasma length becomes 5 cm, which is not as transient dominated as a 2.5 cm case at 600 MeV/m deceleration ($n_0 = 2\times10^{14}\,\mathrm{cm}^{-3}$ plasma) would be.

The simulation results shown in Figure 18 are encouraging, in that a high quality beam obtained by slight variation of the FTF operational parameters, can drive a large plasma wake-field amplitude in the blow-out regime. This is the basic building block needed to construct more complicated experimental arrangements, such as the measurement of the wake-fields with a witness beam and, eventually, the staging of two modules of plasma wake-field acceleration to produce a high quality accelerated beam — the proof-of-principle for the wake-field collider concept discussed in Section II.

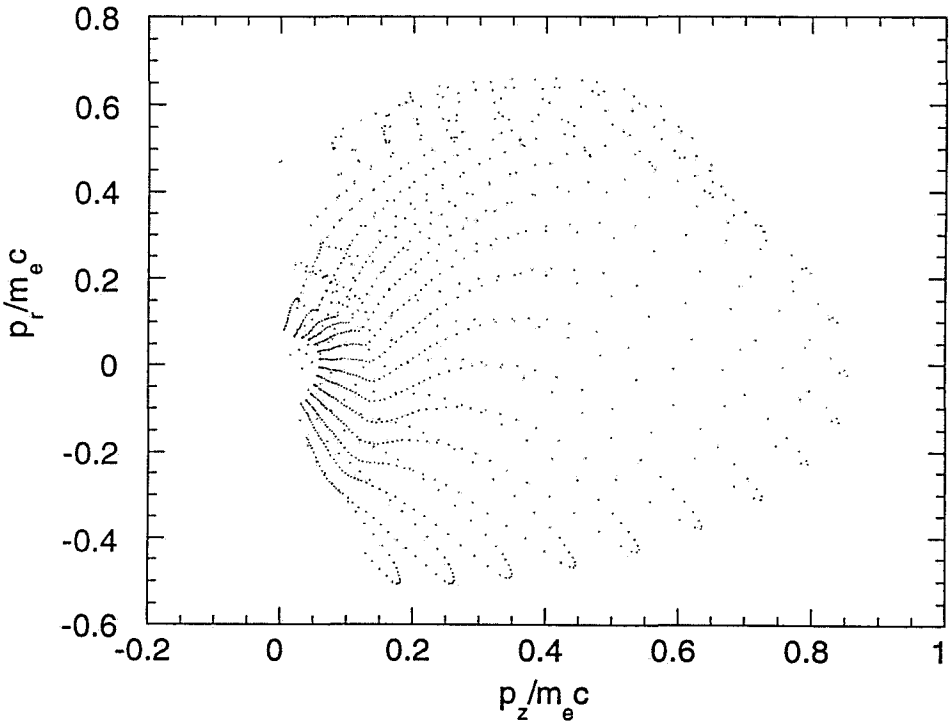

Figure 19. The momentum distribution in the first high density plasma electron region from the simulation of Fig. 1.

In addition to the standard beam diagnostics, one could at FTF implement Compton scattering to diagnose the drive beam energy *in situ* in the plasma, as the scattered photon energy is proportional to the square of the electron energy. This is immediately available at the FTF due to the existence of the University of Rochester high power laser, which is already conceived of as a Compton scattering experimental source. One could also use this laser to diagnose the electron momentum spectrum in the plasma wave, by timing and focusing the laser to intercept the region of the plasma wave near the peak in the accelerating field. This spectrum is moderately relativistic, as is shown in Figure 19. The scattered photons in this case would be detectable by the UCLA VUV detector described in Section III.

4.3 MICROBUNCH CREATION USING PULSE COMPRESSION

The creation of the witness beam from the same rf photoinjector as the drive beam presents some unique problems when a compressor is employed. In order to understand the effects of the compressor on the driving and witness beam pulse lengths and centroid positions, it is useful first to discuss the dynamics of a single bunch. In this case, the most striking effect of the compressor system is timing fluctuation suppression.

The effect of timing fluctuation suppression has been studied extensively in the context of the UCLA photoinjector as implemented in the Neptune Laboratory, which is currently under construction. This laboratory will contain the UCLA photoinjector (presently referred to as Saturnus) and the large, high power carbon dioxide laser, the Mars system. This combined Neptune laboratory system has a high priority experiment, that of the a 100 MeV plasma beatwave accelerator[17] (PBWA) demonstration experiment . In this experiment, the beating of two lines of the Mars laser (10.3 and 10.6 microns) drives a large amplitude plasma wave of 300 microns wavelength. In order to inject a beam short enough to be accelerated with small energy spread into such a system, one must produce

beams much shorter than this length. It is in fact possible to create, as the other application of charge scaling of photoinjector designs, a very short pulse, low emittance beam by compression of the UCLA photoinjector beam. These characteristics are quite attractive for loading of advanced accelerators, as in addition to short bunch lengths and small transverse emittances, the use of a compressor can nearly eliminate the problematic injection jitter associated with the photoinjector drive laser.

The UCLA photoinjector operates at 2856 MHz, but since it consists of a 1.5 cell Brookhaven-style rf gun followed by a short emittance compensating solenoid and a relatively high gradient (45 MV/m peak) 8-cell plane wave-transformer (PWT), it is very close to a scaled version of the TTF photoinjector, and we can apply simple scaling in order to take advantage of all of our work in optimizing the 1300 MHz compressor. The compressor is exactly scaled from the TTF chicane described in previous sections; it has all dimensions scaled by the ratio of the rf wavelengths, magnetic field scaled by the inverse of this ratio, and bend angle and linac rf phase which are left unchanged. In addition, the beam charge is scaled (keeping the beam density constant, but changing only the radial dimension) from the UCLA emittance compensated 1 nC design beam until the bunch length is 2 picosecond FWHM, which is approximately the best achieved by the UV laser presently employed. The beam charge in this case is approximately 33 pC.

Perhaps the most impressive advantage that the compressor adds for use in far IR to mm wavelength advanced accelerators, is that it suppresses injection jitter. This may be a crucial advantage that compressor-based systems offer, and occurs because the compressor maps the bunch centroid to the same longitudinal position to first order in injection phase errors. This suppression is displayed in Fig. 20 which shows the variation in spatial jitter (the difference in position at a given time relative to an external clock) as a function of injection time. The injection jitter is shown in the range of +/-1 picosecond, as is expected from the UCLA photoinjector drive laser. The injection jitter varies approximately linearly, by +/-30 microns (0.1 psec) over this range.

This effect can be understood by recalling that the space charge has changed the effective optimum phase for compression. At the phase which optimally compresses the beam, a zero-charge beam is now overcompressed, which means that the centroid, which behaves as a zero-charge beam now has a first order spatial jitter which is much smaller than (but proportional to) the injection jitter. The suppression of injection jitter is of course dependent on the stability of the rf phase and amplitude in the accelerating structures. If care is not taken to stabilize these quantities, a new source of timing jitter at the output of the compressor will result. It should be noted that if a compressor is used, all produced bunches are in some way partially locked to the rf clock, which is an advantage over laser-based acceleration systems.

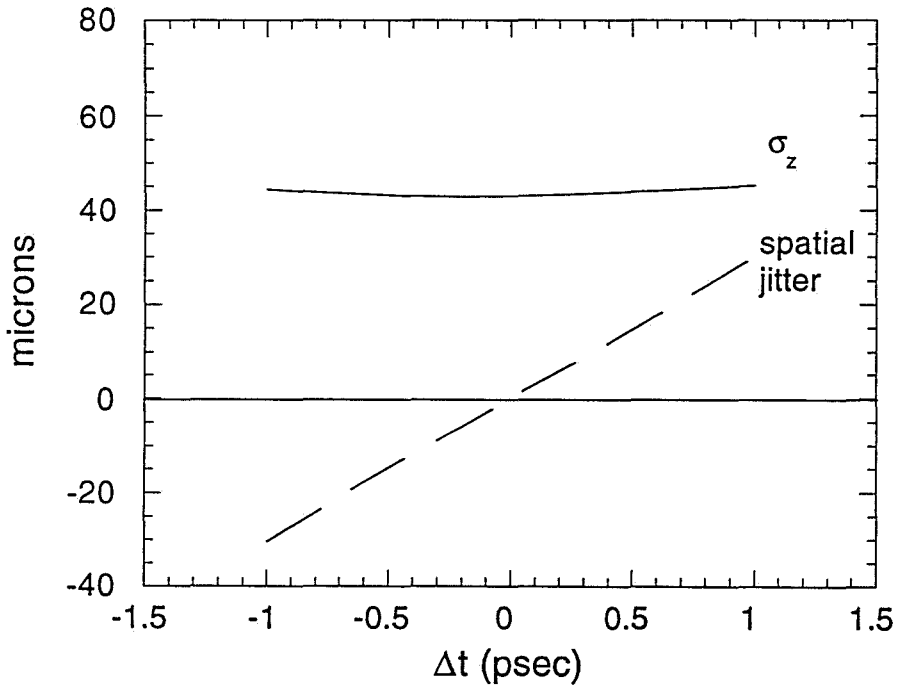

Figure 20. Rms bunch length and longitudinal spatial centroid jitter at compressor end as a function of photocathode cathode laser timing jitter for Neptune photoinjector at UCLA.

For the case of production of two bunches within the photoinjector, the proof-of-principle which was experimentally demonstrated by the measurement shown in Fig. 11, the effects of longitudinal space charge, wake-fields, and rf wave curvature all conspire to make the phase focusing of the compressor system smaller for the witness beam. This is good, because if the phase focusing on the witness beam is not mitigated, then the witness beam would be focused directly onto the drive beam's longitudinal position. This is shown schematically in Figure 21.

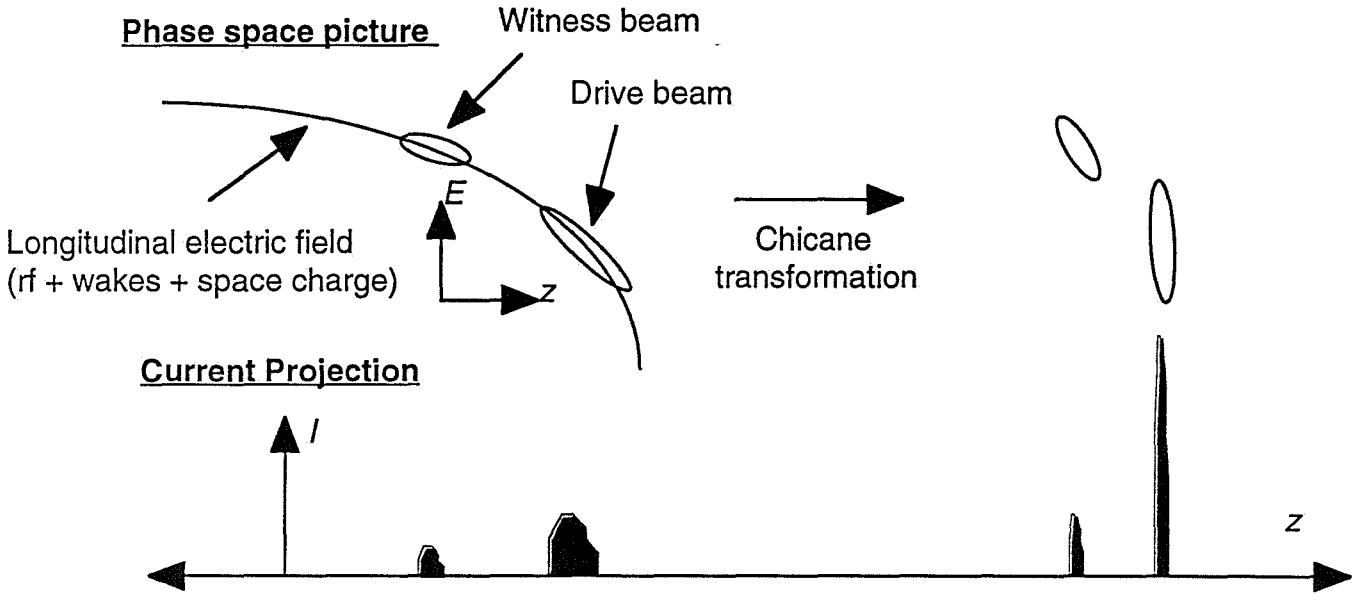

Figure 21. Schematic picture of witness and drive beam creation from the same photoinjector and compressor, showing differential compression of witness and drive beam envelopes and centroids.

There are two effects which are notable here. The first is that, while the drive beam longitudinal envelope is optimally compressed (upright ellipse in phase space), the witness beam envelope is not, due to the curvature of the applied and beam-induced longitudinal electric fields in the photoinjector — the slope of the electric field changes between the two

pulses. This effect is also felt by the beam centroids, as the drive beam centroid jitter (due to laser timing fluctuations) is nearly perfectly canceled, where it is only partially canceled for the witness beam.

While much experimental, computational and analytical work has been performed on this type of photoinjector/compressor system, much work remains. A detailed understanding of the roles played by the space charge and wake-fields, and the ultimate performance of this system, awaits further investigation by computer simulation.

4.4 STAGING OF TWO-MODULE PLASMA WAKE-FIELD EXPERIMENTS

The most compelling advance we hope to make in the proposed experiments at FTF is the staging of two modules of plasma wake-field acceleration, driven off of the same linac *a la* the straw-man collider discussed in Section II. Generation of a high quality accelerated beam from a plasma based accelerator scheme, extendible to ultra-high energy, would represent an important and necessary stride forward in the advanced accelerator field.

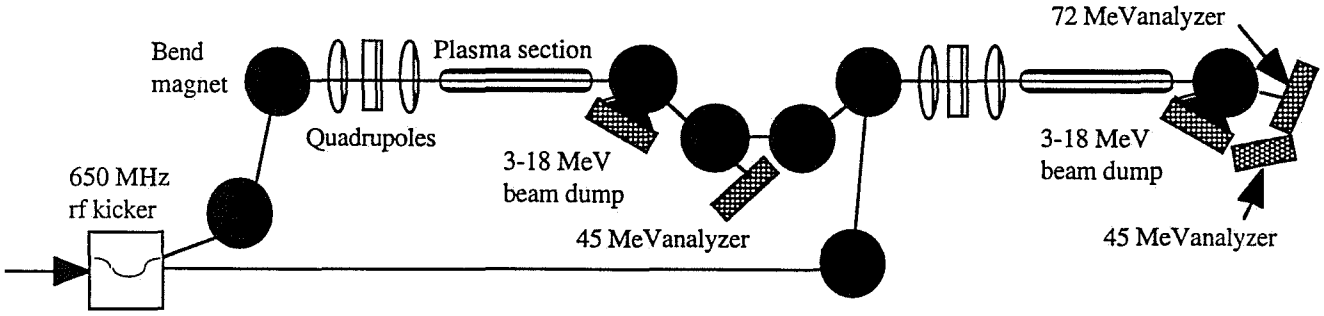

Figure 22. Schematic of two-module plasma wake-field experiment, with rf splitter, two plasma sections, combining optics, beam dumps and energy analyzers shown. Not shown: emittance, pulse length diagnostics.

The extension of a single module experiment to a two-module experiment is shown schematically in Figure 22. The beams are split by a combination of a 650 MHz rf kicker and a static kicker, which allows one drive beam (and its nearby witness) to be kicked into the initial plasma section injection line. It is estimated by scaling a BNL "box" design[18] for a dipole mode cavity to 650 MHz that a differential kick of 6.6 mrad can be obtained with an rf power of 1.3 kW. Downstream of this cavity, the first witness and drive beams are then matched into the plasma focusing channel. After the drive beam loses most of its energy, the plasma is exited and the low energy drive beam is bent into a broad band dump. The same bend magnet feeds the accelerated (45 MeV, effective transformer ratio of 1.5 assumed) beam into a chicane section, which can compress the witness beam further before injection into the subsequent plasma section. The final magnet in the chicane recombines the accelerated beam with a new drive beam and witness beam (used as an ancillary diagnostic in the experiment). At the end of the second plasma module, the beams are bent again, and directed into a low energy beam dump (the drive beam), a 45 MeV energy analyzing array (witness beam 2), and a 72 MeV energy analyzer (witness beam 1).

In this schematic picture, one obviously sees the beam energy diagnostics. Not shown are the emittance diagnostics (pepper pots or slits), which are necessary to show that the accelerated beam is of high quality. There are also plasma diagnostics, beam bunch length diagnostics (coherent transition radiation and/or streak camera based diagnostics, subject to availability) which must be implemented; these are discussed further below.

4.5 PLASMA DEVELOPMENT

While the plasma source in use at ANL is adequate for initial experiments at the FTF, there are a variety of reasons for upgrading it, not the least of which is the eventual need for two sources in the staging experiments. The present source, shown schematically in Figure 8, is a self-heating arc source, which produces a very quiescent and reproducible

plasma. On the other hand, it presents a high heat and gas load to the vacuum system, and the self-heating cathode geometry is quite long and narrow, making the angular acceptance smaller than we would like. In addition, the discharge is DC, and this makes it difficult to place diagnostics within the plasma without degradation for any significant length of time. These problems may be mitigated by the use of a pulsed, externally heated cathode. We plan to test a large bore lanthanum hexaboride tube cathode in this mode soon.

Another serious option for producing such a high density plasma would be an rf resonant heating plasma source. It is envisioned that plasma source and diagnostics development will proceed at both Fermilab and UCLA in the following years, and that the source can be further optimized for our experimental needs.

4.6 BEAM DIAGNOSTICS

In this section we discuss the electron beam diagnostics which we plan to use at the FTF. The choices of diagnostics are driven by the characteristics of the beams we plan to use for the experiments, and by the constraints of the beam transport. The methods we review below have, unless otherwise indicated, been employed in the Saturnus laboratory at UCLA, or in collaborative efforts with the Argonne Wake-field Accelerator and the Fermilab TESLA photoinjector development project. Many are already part of the planned installation at the FTF. It should be noted that all the diagnostics described here give a shot-by-shot response, which is highly useful in photoinjector experimentation due to the fluctuations of the cathode drive laser.

4.6.1. Transverse spot size and position

In order to measure the size (and emittance) of the electron beams which will be employed for much of the FTF program, we must have the ability to measure the beam spot

size at the 40 μm level or above during final focus into high gradient acceleration experiments (20 μm or less for emittance). In the case of transport, we have had experience both at UCLA and ANL successfully measuring beam spots by imaging the (slow) light emission from phosphor screens and from (prompt) Cerenkov and transition radiators. We have achieved a resolution limited, in both cases by CCD camera optics and pixel size, of less than 20 μm. It should be noted that many of the beam diagnostics discussed here rely on digitized video images, which are both acquired by a frame-grabber and analyzed using the Macintosh Labview-based control and data acquisition system.

The UCLA design for the phosphor-based beam spot detector has the phosphor deposited on the downstream side of an aluminum foil mounted normal to the beamline (eliminating depth of focus problems inherent in viewing a plane at an angle), and is viewed by a CCD camera with the aid of a 45 degree front-silvered mirror. Both the phosphor grain size and the expected image bloom due to electron scattering are expected to be less than 10 μm. The phosphor used at UCLA has been calibrated with other measures of beam charge give essentially a linear response (including the camera) over a wide range of incident beam intensities. This linearity has allowed us to make measurements of very small (picoCoulomb) beam charges, such as would be encountered in the witness beams in the proposed experiments, by integrating the light emitted from the phosphor after subtraction of background due to dark current. These phosphor detectors are equipped with precision fiducial markings for calibration of the image sizes, and alignment monuments so that the phosphors may be used as destructive beam position monitors, in that centroid offsets on the screen can be mapped to offsets from beamline center. Phosphor screen assemblies are mounted on remotely controlled actuators, and are viewed at UCLA with cameras equipped with remotely controlled apertures, allowing for considerable change in viewable intensities within a run.

The nondestructive monitoring of beam centroid position is accomplished at UCLA by use of stripline pickup arrays of a Brookhaven design. These arrays of four 50 Ω

striplines allow simultaneous measurement of charge (the sum signal), and horizontal and vertical beam offset (the difference signals).

4.6.2. Beam Charge

The methods for measurement of beam charge are straightforward, and can be classified into destructive and non-destructive. The destructive charge monitors used at UCLA are calibrated phosphor screens, as described above, and Faraday cups. The Faraday cups are of both insertable (mounted on floating remotely controlled actuators) and permanent types. However, the insertable Faraday cup was found in testing at Argonne to be linear in response up to 10 nC; for higher charge the charging of the cup causes unacceptable secondary emission losses. Permanent Faraday cups are located at beam dumps, and are optimized for high capacitance (low charging voltage) and low gamma and neutron radiation production. Faraday cups are terminated with high (1 MΩ) impedance for short pulse integrated charge measurements, and low (50 Ω) impedance for average current (*e.g.* dark current) measurements on the microsecond scale.

The nondestructive charge measurement systems employed at UCLA and ANL are the stripline sum signal described above, and an integrating current transformer. The integrating current transformer is a capacitively terminated, ferrite-loaded toroid which is mounted over a ceramic DC break in the beamline. It integrates the current over approximately a nanosecond and outputs a ten nanosecond pulse whose charge (and peak current) is proportional to the beam charge. This signal is acquired using a charge integrating ADC on a shot-by-shot basis.

4.6.3. Transverse emittance

One of the most difficult quantities to measure in an ultra-high brightness, low energy electron beam is the transverse emittance. This is because the behavior of the beam

is controlled by the space charge during most of its propagation. For this reason, linear methods such as quadrupole scans do not easily provide unambiguous measurements of the "thermal" nature of the beam - the spread in transverse velocities which give rise to a finite emittance. Given these considerations, we have developed a slit-based emittance measurement system which is now employed at UCLA and in the TESLA injector experiments at ANL. The purpose of collimating the high intensity electron beam with slits in these devices is two-fold. The first purpose is of course to separate the beam into many beamlets, whose intensity distribution at some downstream point can be measured to give the phase space distribution of the beam; the width of each beamlet gives a measure of the width of the transverse momentum distribution at each slit, and the centroid of the beamlets gives the correlated offset of the momentum distribution at each slit. The second is to mitigate the space-charge effects in the beam by removal of most of the beam charge, so that the beamlets are thermal emittance dominated.

For the moderate energies found in the planned beamlines (15-55 MeV), the high brightness beams are space-charge dominated except near small waists. Collimation with slits mitigates this situation, however, by creating low current, small σ_x beamlets which have the same uncorrelated "temperature" as the original beam. For the FTF photoinjector, it is acceptable to have $d = 25 - 50\ \mu m$ slits in order to obtain beamlets which are emittance dominated, and these have been implemented at UCLA and at ANL on the TTF photoinjector experiments. There are, in fact, other design considerations which impacted the choice of slit width, having to do with the angular acceptance of the slits. The depth of the material used to intercept the beam is dictated by our desire to either stop the beam or scatter it sufficiently so that it doesn't affect the measurement of the nonintercepted beamlets. Typically, 1-2 mm of tungsten will produce this effects at 18 MeV. Once this length has been chosen, one can examine the angular acceptance of the slits. The first thing one needs to do is to specify an rms beam angle associated with the finite beam emittance, which assuming we place the slits at a waist, is $\phi = \varepsilon_n / \gamma\sigma_0$. An additional problem in

measuring angular distributions can arise due to slit scattering. For the relatively large angles we are dealing with in these measurements, slit scattering is not an important effect.

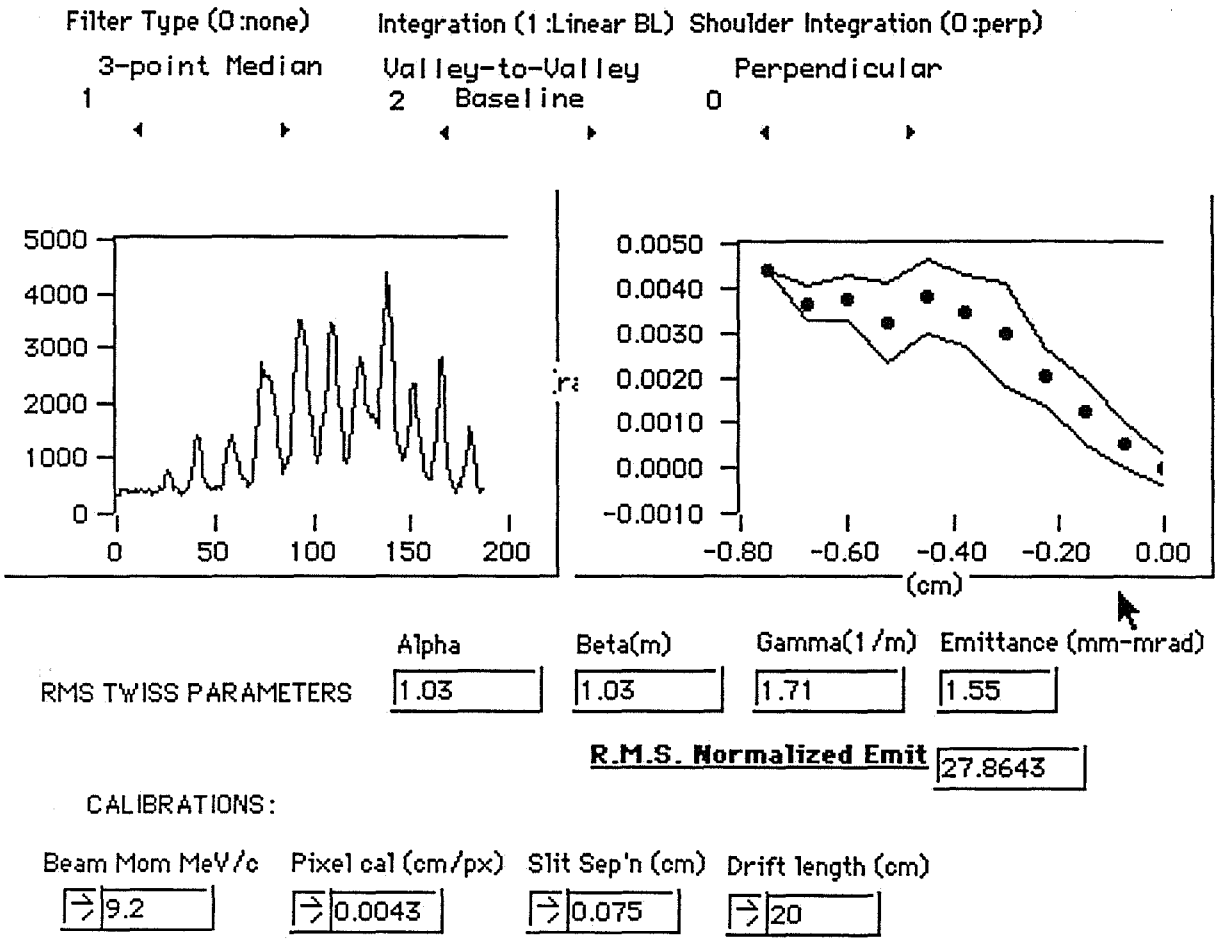

Figure 23. Labview virtual instrument panel for measuring rms emittance with slits.

The slit separation w is chosen to be much larger than the slit width d and smaller than the beam size, to ensure that we can resolve the beam. In the UCLA case, the slit width is taken to be 0.75 mm. This width must also be consistent with not allowing the beamlets to overlap at the detecting phosphor, a condition which depends on the distance of the drift to the phosphor L_d. Care has been taken in the machining specifications for the

slits, to ensure that they are flat over the entire surface parallel to the beam propagation. This is accomplished by electron discharge machining (EDM), and is essential for the UCLA systems (and others developed for Argonne and Fermilab which have even narrower slit requirements). The slits are mounted on a rotatable-insertable actuator which is driven by a stepping motor with a step-down 100:1 gear, which allow fine to alignment of the slits.

An example of the measurements made this on a 9.2 MeV beam which had a large emittance due to filamentary emission at the cathode is shown in Figure 23. The algorithm in the Labview virtual instrument calculates from the centroids and full width-half maxima of the beamlets all of the rms Twiss parameters ($\alpha, \beta, \gamma, \varepsilon$), using an rms equivalent obtained by assuming each beamlet is thermal. This is important, because we have implemented an algorithm in PARMELA which also calculates the rms phase space moments in this manner - what we term "measurement" emittance. In this way, we remove much of the ambiguity in the comparison of simulation and experiment.

IV. Longitudinal beam profile

The longitudinal profile of the beam at the UCLA and AWA photoinjector has been measured using detection of beam-derived Cerenkov photons from quartz plates, imaged by a streak camera to give information about the longitudinal profile of the beam. The use of a solid Cerenkov emitter implies large Cerenkov angle, non-negligible electron scattering effects, depth of focus problems and an inherent resolution of several picoseconds. This technique, as well as the use of transition radiation at the ANL experiments, has been useful for measuring bunch lengths many picoseconds long, as well as performing time dependent imaging in plasma lens experiments. We have just begun the testing of aerogel, which has been obtained from the Caltech Jet Propulsion Laboratory, as a Cerenkov radiator. We are attracted to aerogel as a compromise between a solid and gas medium.

Solids are unacceptable both because of the difficulty of using the wide-angle of photon emission, preservation of time information, and because the Coulomb scattering in the medium cause the beamlet images (which should be resolvable at the 10-20 micron level) to bloom. There is of course no bloom if we employ optical transition radiation, but the signal is too low to use for many applications. Gas cells, which have been used in previous streak camera imaging experiments at Argonne, are likewise problematic because many of the measurements will have to be performed below threshold for Cerenkov radiation. In order to lower the threshold, we must pressurize the gas cell, which in addition to making a more complicated design generally forces use of an entrance window which gives unacceptable scattering and image bloom. Aerogel allows us to choose the index of refraction to optimize the Cerenkov angle, number of photons, thickness of the radiator, etc.

The use of a streak camera to give information about the longitudinal profile of the beam has resolution practically limited to a picosecond or two, and the camera is very expensive (~$200k). There are, however, many physical situations encountered in rf photoinjector-based experiments where one needs resolution better than this, and where the imaging of one transverse distribution is not needed. In the past few years, the use of coherent transition radiation (CTR) has become more common for these types of experiments. This type of device is presently under construction by a collaboration between UCLA and Prof. Uwe Happek of the University of Georgia. The monochromator in this case is a scanning polarizing Michelson interferometer, and uses Golay cell detectors, whose response is nearly flat over the frequency range of interest. This design has been optimized over the last few years by Prof. Happek, who has worked with Cornell, Vanderbilt, and CEBAF on this measurement technique, and has diagnosed 300 micron rms bunch lengths with it. This technique has been used by Wiedemann, *et al.*, to measure sub-100 micron bunches at Stanford.

V. PROPOSED EXPERIMENT -SUMMARY AND PLAN

5.1 GOALS

In summary, the goals of the proposed program in plasma wake-field acceleration are as follows:

1. Demonstration of High Gradient Acceleration

A primary goal of this experiment is to demonstrate the achievement of an accelerating gradient in the range of 1 GeV/m, using a single bunch of rf photoinjector-derived beam with a compressor, to drive a of plasma into a nonlinear response. The plasma wake-fields in this nonlinear "blowout" regime will be measured with the aid of a low charge, variable in relative timing with respect to the drive beam, witness beam, which will derived from the same photoinjector/compressor. These results are expected to verify scaling of plasma wake-fields with plasma density, beam charge, bunch length, and emittance and drive bunch parameters in a single stage. Emphasis will be placed on complete diagnosis of the plasma wave, energy transfer between the wave and the driving and witness beams evolution and on phase space characterization of the witness beam.

2. Beam Quality Preservation

Another important goal is the demonstration of high gradient acceleration of a low emittance beam, *i.e.* the preservation of the injected witness beam emittance. This issue is of primary importance for determining the feasibility of short wavelength, high gradient

advanced accelerator schemes. It has, to date, been left unexamined experimentally; a thorough study will be made of the mechanisms which affect emittance growth.

3: Staging - A Road to an HEP Collider

Finally, the issue of staging multiple accelerating modules will be investigated, as this is crucial to the viability of an accelerator of relevance to HEP. Questions concerning beam merging techniques, synchronization and emittance preservation along a multiple-stage accelerator will be considered. This demonstration would allow the type of collider discussed in Section II to be more seriously considered in planning for future high energy lepton linear colliders.

5.2 Required Resources

The most costly aspect of this experiment is the photoinjector, which is already under construction. Thus the incremental cost of the accelerator test is rather minimal. However, it should be noted that several parts of the photoinjector are scheduled for shipment to DESY early in the project and as such will have to be replaced for long-term use in the accelerator test. These include the rf gun and one of the rf modulators, along with minor components of the beam optics. Of these items, the rf modulators represent the largest expenditure that will be needed. Options for the use of the current modulators are described below.

The accelerator test project at A0 requires the use of two short-pulse high-power rf systems: one is used to power the rf gun for production of short electron bunches, while the second is used to accelerate the bunches to up to 20 MeV in a linac. In both cases the sources may be short pulse (<100 msec), and in the 2-10 MW range, depending on the type of linac employed. The sources consist of power tubes (klystrons) and modulators,

which in turn require pulse transformers and capacitors of the appropriate energy storage capacity.

Currently, two complete modulators are being fabricated for use at DESY, and at least one of these is planned to be shipped to DESY within approximately one year. In addition, a Boeing modulator is available at Fermilab, though retrofitting of this modulator will be required. Moreover, a number of relatively long pulse (100 μsec) moderate power (6 MW) klystrons, and some of the parts necessary for additional modulators exist at UCLA, which may be used to construct additional systems.

However, it is also feasible and desireable for a number of programmatic reasons to employ a longer-pulse, but lower power, rf system, which will be required for the superconducting cavity which is now under construction. Given the development program already in place at A0 for a superconducting cavity, the programmmatic constraints of the modulator fabrication and delivery to DESY, and the primary goal of testing a system most like TTF photoinjector at A0, the following options present themselves (in descending order of desirability):

1. Proceed with the superconducting cavity development at A0 which will require the use of a long-pulse, low-power rf system already available at Fermilab. In addition, keep the second high-power modulator at Fermilab for the normal conducting rf gun. In this option, the photoinjector at Fermilab is kept operational throughout the next several years by a staged use of the low-duty factor gun currently at ANL, followed by the DESY prototype now beginning construction, in conjunction with one of the DESY modulators.

As this option is the most desirable, we show proposed timeline for including near-term use of the DESY modulators in Fig. 24.

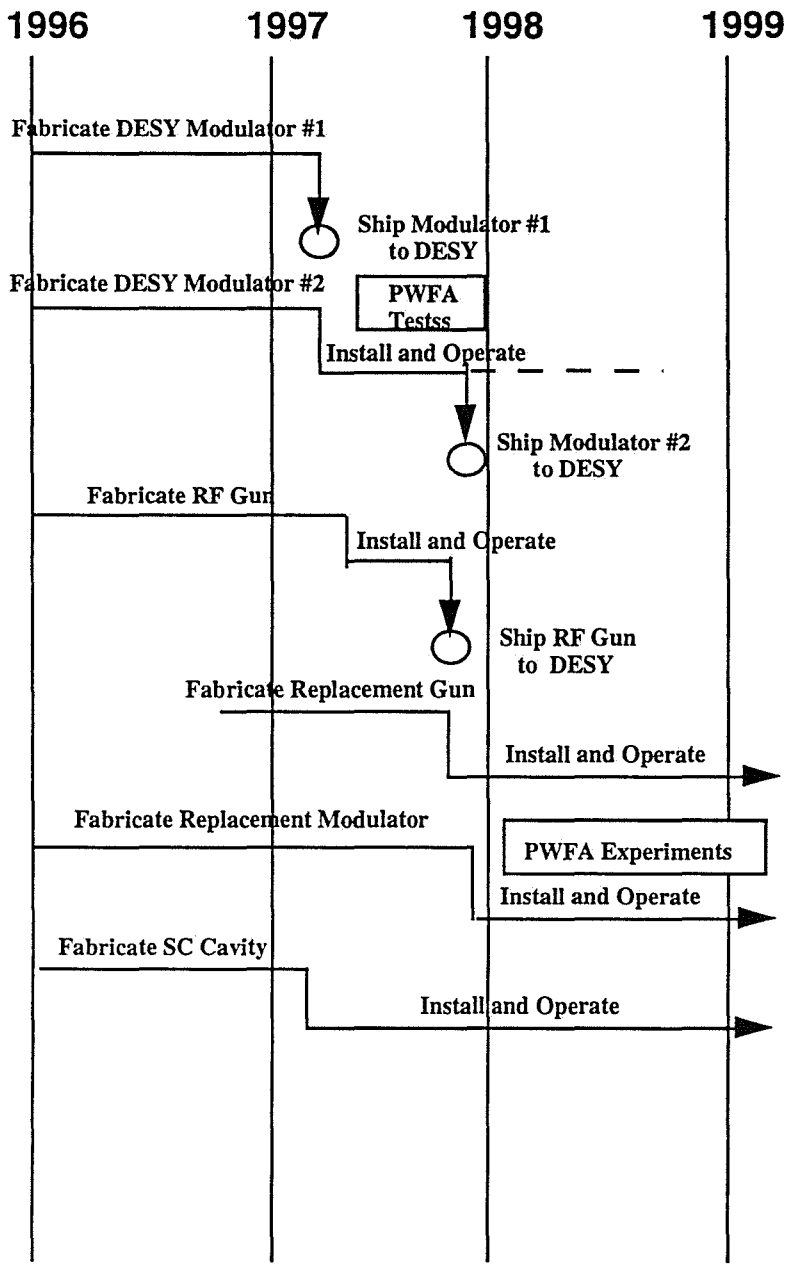

Figure 24. Timeline for staged plasma wake-field experiments at the FTF for rf option 1, superconducting linac.

2. A variation of this plan is required if the superconducting cavity cannot be developed at Fermilab. It is then necessary to simultaneously retrofit the Boeing modulator (or construct a new modulator) and use the normal conducting linac presently in use at ANL, driven by a

UCLA klystron. The second modulator would not be shipped to DESY until the replacement systems are available at Fermilab.

3. A third option, which completely avoids the use of the DESY modulators, is to construct new, relatively short pulse (< 20 msec) modulators and use klystrons and parts available both at UCLA and FNAL. This will require the purchase of additional components, though the cost, commensurate with the small requirements of pulse length and duty cycle, is expected to be modest. In order to permit timely use of these modulators, construction would need to commence in the near future. This option, while clearly showing the least continuity and poorest match to the FTF/A0 program as it is presently conceived, does give the minimally required accelerating system at a relatively low cost.

It should be made clear that the primary option being proposed is the number one, as this most smoothly meshes into the current development program for the DESY photoinjector.

5.3 Required Beam Performance: Infrastructure Demands

The required beam parameters as described in Section IV are summarized in Table 4.1. According to simulations of the beam dynamics with PARMELA, as well as integrated PIC simulations fo the plasma response, these parameters are easily attainable using the FTF photoinjector hardware, including the laser. In many ways, since these experiments require less in both the specifications of rf pulse lengh (the most demanding aspect of the cavity design) and the number of pulses per rf fill (the most demanding aspect of the laser design), the performance of the entire system can be derated from the TTF specifications. In addition, the existence of a high peak power, picosecond laser (from Univ. of Rochester), allows us to consider implementation of advanced beam and plasma wave

diagnostics at an incremental cost. Thus the plasma wake-field program can be seen to fit well with both the existing hardware and the goals of the FTF collaboration.

5.4 Required Resources and Collaboration

This project, as a subset of the FTF collaboration work, is to be carried out as a collaboration between Fermilab, UCLA and the University of Rochester. As already mentioned, this work benefits from the ongoing construction of a short-bunch electron photoinjector at Fermilab, which has been undertaken in collaboration with UCLA and University of Rochester personnel. This arrangement is expected to continue as the photoinjector is brought into operation and is readied for a variety of experimental applications. In addition, UCLA will scale up its present effort, providing personnel and hardware support. The following is a summary of expected participation.

The advanced accelerator test at A0 is being carried out in two phases. The first is the design and construction of a high intensity photoelectron source, including rf power sources, superconducting cavity and control systems, which will be used as the prototype for the TTF injector at DESY. The second phase will follow testing of the photoinjector at Fermilab and will consist of the implementation of the appropriate beam optics, diagnostics and plasma test chamber for the prototype accelerator. An extended research and development period will follow the initial construction phase.

5.4.1 Personnel, Phase I

In the first phase, the TTF photoinjector is being constructed under a collaboration with the University of Rochester, UCLA and DESY. The following personnel are involved in the construction effort and/or the testing of the initial TTF photoinjector at ANL:

H. Edwards	Fermilab	50%
F. Nezrick	Fermilab	50%
P. Colestock	Fermilab	50%
K. Koepke	Fermilab	50%
A. Fry (student)	Univ. of Rochester	100%
M. Fitch (student)	Univ. of Rochester	100%
E. Colby (student)	UCLA	100%
M. Conde	UCLA	50%
J. Rosenzweig	UCLA	20%
A. Melissinos	Univ. of Rochester	50%
B. Taylor (engineer)	University of Rochester	100%
N. Bigelow	University of Rochester	20%
Post Doc (to be hired)	Fermilab	100%

Table 5.1. Personnel for the initial phase of FTF construction

Drafting, technician and engineering Support for the FTF and associated projects have been mainly provided by Fermilab, with some contribution coming from the universities in terms of fabricated components.

5.4.2 PERSONNEL, PHASE II

In the second phase, Fermilab is committed to carrying out the R&D required on the test accelerator at A0, as an initial commisioning of the TTF photoinjector, along with other physics experiments based on the availability of the short pulse photoinjector. The following personnel are anticipated to be involved:

P. Colestock	Fermilab	100%
B. Noble	Fermilab	50%
J. Rosenzweig	UCLA	50%
L. Serafini	INFN-Milano	25%
A. Melissinos	Univ. of Rochester	10%
F. Nezrick	Fermilab	20%
Nick Barov (Post-doc)	UCLA	100%
Post Doc (to be hired)	Fermilab	100%
Post Doc (to be hired)	Fermilab	100%
Post Doc (to be hired)	Fermilab (Phase I)	100%
M. Fitch (student)	Univ. of Rochester	100%
New Student (to be hired)	Fermilab	100%
New Student (to be hired)	UCLA	100%
B. Taylor (engineer)	Univ. of Rochester	100%

Table 5.2. Personnel for the second phase of FTF activities, in support of the plasma wake-field experimental program.

Again, it is anticipated that much of the technical support for this stage of the project will come from from Fermilab. In the following section, we will outline the estimated incremental hardware costs associated with the project, as well as the expected UCLA in-kind contributions to this cost.

5.4.3 HARDWARE COST ESTIMATE

The following table contains a summary of the incremental (not including any costs which are needed to completer the FTF itself) hardware cost associated with this three-to-four year project, followed by a short discussion of the items on the list, their priority and expected origin.

ITEM	COST ($k)	UCLA CONTRIBUTION
Plasma Source(s)	65	25*
Plasma Diagnostics	35	20*
Vacuum Pumps	50	20*
Beam Optics Magnets	60	60
Magnet power supplies	55	15
Beam pipes, other vacuum	50	10*
Transverse beam diagnostics	40	18
CTR diagnostics	22	22
Electron spectrometers	45	30
Beam position monitors	40	—
Data acquistion, computers	50	20*
Laser optics	23	—
Video cameras	15	6
650 MHz cavity, source	45	—
Streak camera	(175)	—
X-ray and VUV detection	25	14*
TOTALS	620 (795)	260 (*109)

Table 5.3. Estimated incremental cost, with UCLA in-kind contribution, of the staged plasma wake-field acceleration experiment. The totals include the possible inclusion of a streak camera, which is a major expense for FNAL. The items indicated with a * are existing UCLA equipment which will be moved from ANL and UCLA.

Several observations are motivated by this list. The first is that the incremental cost to Fermilab is quite low, especially when normalized to the cost of FTF itself. The second is that the total in parentheses includes the possible inclusion of a streak camera, which is a major expense for FNAL. This piece of experimental infrastructure is motivatable by application to the FTF photoinjector diagnosis alone, and has been proven to be extremely valuable in photoinjector, laser-plasma and beam-plasma work at ANL and UCLA; it is strongly recommended. The items indicated with a * are incremental to the FTF, but not to UCLA, as they are existing UCLA equipment which will be moved from ANL and UCLA to FNAL. Also, it can be seen that much of the major new equipment costs for UCLA are in the dipole, quadrupole, steering and spectrometer magnets. These items are to be constructed in a magnetics fabrication lab in the physics department at UCLA, and will be on permanent assignment to the FTF. Other optical components will be supplied by the University of Rochester as required.

If the lowest cost scenario is adopted (no streak camera), then the incremental cost (for new equipment) to UCLA is about $150k, and to Fermilab is $360k. These numbers are quite small for the multiyear program, because we have left out all of the costs of the experiment which are the needed in any case for the commissioning of the FTF itself. This experimental program is heavily leveraged in the funding; most of the investment needed from Fermilab is already committed.

REFERENCES

1."Acceleration and Focusing of Electrons in Two-Dimensional Nonlinear Plasma Wake-fields", J. B. Rosenzweig, *et al., Phys. Rev. A -- Rapid Comm* . **44**, R6189 (1991).

2. B.N. Breizman, *et al.,* Univ. of Texas Fusion Institute Preprint (1991).

3. K. Bane, *et al., IEEE Trans. Nucl. Sci* **32,** 3524 (1985).

4. "Propagation of Short Electron Pulses in an Underdense Plasma", N. Barov and J.B. Rosenzweig, *Phys. Rev. E* **49** 4407 (1994).

5. D. Whittum, *et al., Phys. Rev. Lett.* **67** (1991).

6. "Transverse Stability of the Primary Beam in the Plasma Wake-field Accelerator, J. Krall and G. Joyce, *Advanced Accelerator Concepts* 505 (AIP Conf. Proc. 335, 1995).

7. W. Gai, *Advanced Accelerator Concepts,* (AIP Conf. Proc. , 1990).

8. Z. Huang, P.Chen and R.D.Ruth, *Phys. Rev. Lett.* **?** ?(1996).

9. "Channeling and Stability of Laser Pulses in Plasmas, P. Sprangle, *et al.*, 163, (AIP Conf. Proc. 335, 1995).

10. "Laser Acceleration", W. B. Mori, T. Katsouleas 112 (AIP Conf. Proc. 335, 1995)

11. 10. J.B. Rosenzweig, "Particle Wake-field Accelerators," Proceedings of the 1992 Linear Accelerator Conference, 835 (AECL-10728, Chalk River, 1993).

12. J.B. Rosenzweig, *et al., Phys. Rev. Letterss* **61**, 98 (1988), J. B. Rosenzweig, *et al., Phys. Rev. A - Rapid Comm.* **39**, 1586 (1989), J.B. Rosenzweig, *et al,, Phys.*

13. "Measurement of Plasma Wake-fields in the Blow-out Regime", N. Barov, M. Conde, and J.B. Rosenzweig, in the *Proceedings of the 1995 Particle Accelerator Concerence,* 631 (IEEE, 1995).

14. "Pulse Compression in Radio Frequency Photoinjectors - Applications to Advanced Accelerators", J.B. Rosenzweig, N. Barov and E. Colby, *IEEE Trans. Plasma Sci.* **24**, 409 (1996).

15. "Charge and Wavelength Scaling of RF Photoinjector Designs", J.B. Rosenzweig and E. Colby, *Advanced Accelerator Concepts* p. 724 (AIP Conf. Proc. 335, 1995).

16. "Charge and Wavelength Scaling of RF Photoinjectors: A Design Tool", J.B. Rosenzweig and E. Colby, in the *Proceedings of the 1995 Particle Accelerator Concference* 957 (Dallas, 1995).

17. C.E. Clayton, *et al., Phys. Rev. Lett.* **70**, 37 (1993).

18. X.Wang, *et al, Nucl. Instr. Methods A* **356**, 159 (1995).